

Supplementary Methods

1. Processing of targeted methylation NGS data

Data were processed using fastqc to assess quality and read through adapters were trimmed using Trimmomatic v0.36. Since DNA was bisulfite treated, we aligned the reads based on three nucleotides (thymine(T), adenosine(A), guanine(G)) to the human genome (hg)19 using the BSMAP v2.90 (1, 2). The duplicated reads were removed with Picard tools v2.1.0 (<http://broadinstitute.github.io/picard>), and unaligned reads were clipped (hard-clipped) using the bamUtil 1.0.13(3).

The CpG methylation ratio of each loci was calculated using formula (1), which takes cytosine(C) and thymidine(T) counts from all reads covering each CpG loci.

$$\text{Methylation Ratio} = \frac{c}{c+t} \quad (1)$$

From all sites included in our predesigned capture panel (Roche Nimblegen SeqCap EpiGiant), only sites with a minimum coverage of 10X were considered for further analysis of CpG (**Supplementary Fig. S1**).

The methylation ratio was computed using the methylKit R package v1.6.2(4).

2. Selection of optimal data inputs for PCA

Adjacent CpG methylation levels are usually highly related, and previously studies have demonstrated high sensitivity of identifying tissue-specific methylation markers using sliding window approaches (5-7). Here we combined adjacent CpG sites into methylation segments of fixed length, and the median methylation ratio across all CpGs within the segment was used to represent the methylation ratio of the segment using methylKit R package v1.6.2(4). Initially we used 100bps with sliding window of 50bps and generated > 1.47 million windows across all CpGs in our target panel. We applied principal component analysis (PCA) using the FactoMineR v1.41 package.

To eliminate potential biases due to the selection of segmentation length, we optimised the segmentation length parameter. To do so, we tested segments of 10bps, 100bps, 1000bps and 10,000bps with sliding windows of 5bps, 50 bps, 500 bps and 5000 bps, respectively. We found that the smaller the window size, the more data we had to drop when combining plasma samples due to variable inputs and sequencing coverage (**Supplementary Fig S19**). We also found that the methylation ratio of 100bps segments with 50 bps sliding window shows high consistency with the methylation ratio estimated at single CpG level (**Supplemental Fig S20**). The correlation of PC1 with genomically-determined tumor fraction was >90% regardless of window sizes (**Supplementary fig. S21**).

Thus, to preserve more detailed methylation information, and to guarantee successful execution in a reasonable amount of time, the setting of 100bps segments with 50 bps sliding window was applied for the rest of our analysis. The setting in our study does not represent the overall best solution, but we presented a framework that is the most suitable for the samples we analysed.

3. Analysis of low passage whole genome bisulfite sequencing (LP-WGBS) data

Reads from LP-WGBS were processed as high coverage NGS. To calculate PC1 values derived from LP-WGBS, we used the default segmentation length of 100 bps and calculated the methylation ratio of each segment based on formula (I). To maximize the available information obtained from our data, we imputed methylation data from higher coverage bisulfite data based regularised iterative PCA algorithm (8) (missMDA R package (v1.13)), and projected on the PCA model as described above. The regularisation process with random initialisation can also circumvent the over-fitting problem, which might reduce the generalization capabilities of our findings.

4. Low-passage whole genome sequencing

Low-passage whole genome sequencing (LP-WGS) on both bisulfite-treated and untreated plasma DNA was performed with a target 1x coverage. For each sample, reads from LP-WGS on untreated plasma DNA were aligned to the hg19 using BWA-MEM version 0.7.12-r1039 and de-duplicated using Picard tools v2.1.0. The human genome was then divided into non-overlapping bins of 1 million base pairs, and, for each sample, the de-duplicated reads were counted per bin using HMM Copy (<http://compbio.bccrc.ca/software/hmmcopy/>) (9). Next, ichorCNA (<https://github.com/broadinstitute/ichorCNA>) was applied to estimate the tumor content of each sample (10). The algorithm first, removed bins in the centromere regions, with a flanking region of 100,000 base pairs. For all the remaining bins read counts were corrected by GC content and mappability issues. The normalised read counts were then fed into the Hidden Markov model (HMM), which is a probabilistic model assigning each bin into one possible state (hemizygous deletions (HETD, 1 copy), copy neutral (NEUT, 2 copies), copy gain (GAIN, 3 copies), amplification (AMP, 4 copies), and high-level amplification (HLAMP, 5 or more copies). Based on the copy number profile, the model estimated a ploidy and tumor content for every sample. Finally, the algorithm was initiated with ploidy values 2 and 3, and normal fraction, which is 1 minus tumor fraction of 0.0, 0.1, 0.2, 0.3, 0.4, 0.5, 0.6, 0.7, 0.8, 0.9, 0.95. The solution with maximum likelihood among all of these initial combinations was automatically assigned. The CNA status was estimated based on the logR values of each 1Mbp region obtained by the ichorCNA analysis with fixed threshold of 0.5 (GAIN: $\log R \geq 0.5$, LOSS: $\log R \leq 0.5$).

5. Methylation Signatures by Principal Component Analysis (PCA)

We applied unscaled PCA using FactoMineR (<http://factominer.free.fr>) (11). The PCA model comes with the eigenvector, eigenvalues and correlation matrix comprised of correlation coefficient by each segment. We plotted the distribution of the top-K highly correlated segments based on the correlation matrix returned by PCA, and these segments were highly representative of each eigenvector (e.g., principal component 1, or PC1). To identify the optimal value K of highly correlated segments, we tested multiple K values equal to 10, 100, 1,000, and 10,000 and calculate intra-sample variance, and the correlation between median methylation ratio with genomically-determined tumor fraction (**Supplementary Fig S5 and S6**).

6. Gaussian Mixture Model (GMM)

Methylation ratio of ct-MethSig segments derived from LNCaP cell lines, and healthy volunteer plasma were extracted. To estimate the probability density function (pdf), we applied kernel density estimation (kde), assuming a mixture of two Gaussian distributions consistent with the input dataset of normal prostate epithelium (**Fig. 6**). The Gaussian mixture model (see formula II) applies expectation-maximization (EM) to fit the mixtures of Gaussian distributions by an iterative process (12). In our experimentation, the model was executed with maximum iterations of 100 times and 'k-means' method for initialization, and we hypothesized that there were two Gaussian distributions, each of them with its own general covariance. The Gaussian mixture model was subject to cross-validation on random split set of regions over 100 times to prove the robustness of the approach (**Supplementary Fig S22**). The fitted GMM (number of class = 2) was then used to predict ct-MethSig segments of prostate epithelium (PrEC) (13).

Gaussian mixture model: $g_j(x) = \Phi_{\theta_j}(x)$; where $\theta_j = (\mu_i, \sigma_j^2)$ (II)

7. Analysis of Illumina HumanMethylation450 BeadChip dataset

The microarray processed data were obtained from the Gene Expression Omnibus (14) repository (GSE84043). From the dataset we selected the probes overlapping with MethSig1 segments. The methylation ratio of each segment was obtained considering the median of the β values of the overlapping probes. The tumor fraction estimates by different methods were obtained by the sample information published (15).

8. Statistical Analyses

8.1 Methylation ratio difference with Kruskal-Wallis and Dunn's test

The samples were grouped based on tissue of origin and clinical status (white blood cells, plasma healthy volunteer, plasma baseline and plasma progression). Samples were grouped by ct-MethSig and AR-MethSig, and the median methylation ratio of each 100bp segment was estimated in each group of samples. To keep the analysis consistent, we considered only segments present in all samples (340,467 segments). All the selected segments were split in two groups based on the overlap with the promoter region of known genes (263,262 non-promoter segments, 77,205 promoter segments). The promoter region was defined as 1k base-pair upstream and downstream of the transcription start site (TSS). The significance of the differences among each group was calculated using Kruskal-Wallis test (one-way ANOVA on ranks) as implemented in the R v3.4.0 (<https://www.R-project.org> (2018)) stats package. After we defined the significance of the differences, we assessed the difference of the methylation ratio across each group using the Dunn's test as implemented in FSA R package v0.8.22 (<https://github.com/droglenc/FSA>).

8.2 Correlation and association analysis

Correlation analyses of continuous measures were performed using the Pearson correlation method as implemented in the R v3.4.0 stats package. The association analysis between principal components and CNA of each region was performed by grouping the principal component values of each sample based on the CNA observed for the region (LOSS, NEUTRAL and GAIN). The differences in the principal component values distribution among groups was then assessed using the Kruskal-Wallis test (one-way ANOVA on ranks) as implemented in the R v3.4.0 stats package.

8.3 Functional enrichment analysis

Functional enrichment analysis (chemical and genetic perturbations, MSigDB) was executed using the enrich R package (v0.1) based on all the MSigDB main categories (MSigDB database v6.0) (16) with a significance threshold of 0.05 on Benjamini corrected p values.

8.4 Motif enrichment analysis

Motif enrichment analysis was used to identify potential transcriptomic regulators of methylation signatures (MethSig). The start of MethSig top 1000 correlated segments were submitted to find the possible motif binding sequences over-represented as compared to the default background set (17). The pipeline (Pscan-Chip) (17) originally designed for the analysis of chromatin immunoprecipitation followed by next generation sequencing technologies was applied. The program automatically scanned 75 bps preceding and after the 'peak' regions that we submitted with controlled background, and known transcriptional factor binding motifs obtained from JASPAR version 2018. Local enrichment p-value was two-tailed and denoted whether the motif was over-represented in the 150-bp region compared to the genomic regions flanking them. Global enrichment denoted whether the motif binding sequence was over-represented in the region with respect to global background composed of pan-genome putative regulatory regions from various cell lines. We performed the analysis on top highly correlated segments with PC1 or PC3 and other randomly selected regions from our custom, targeted enrichment panel. The result of ar-MethSig was validated by an orthogonal pipeline (18), and the finding was consistent to original approach as described above (data not shown).

References

1. Xi Y, and Li W. BSMAP: whole genome bisulfite sequence MAPping program. *BMC Bioinformatics*. 2009;10:232.
2. Bolger AM, Lohse M, and Usadel B. Trimmomatic: a flexible trimmer for Illumina sequence data. *Bioinformatics*. 2014;30(15):2114-20.
3. Jun G, Wing MK, Abecasis GR, and Kang HM. An efficient and scalable analysis framework for variant extraction and refinement from population-scale DNA sequence data. *Genome Res*. 2015;25(6):918-25.
4. Akalin A, Kormaksson M, Li S, Garrett-Bakelman FE, Figueroa ME, Melnick A, et al. methylKit: a comprehensive R package for the analysis of genome-wide DNA methylation profiles. *Genome Biol*. 2012;13(10):R87.
5. Lehmann-Werman R, Neiman D, Zemmour H, Moss J, Magenheimer J, Vaknin-Dembinsky A, et al. Identification of tissue-specific cell death using methylation patterns of circulating DNA. *Proc Natl Acad Sci U S A*. 2016;113(13):E1826-34.
6. Guo S, Diep D, Plongthongkum N, Fung HL, Zhang K, and Zhang K. Identification of methylation haplotype blocks aids in deconvolution of heterogeneous tissue samples and tumor tissue-of-origin mapping from plasma DNA. *Nat Genet*. 2017;49(4):635-42.
7. Sun K, Jiang P, Chan KC, Wong J, Cheng YK, Liang RH, et al. Plasma DNA tissue mapping by genome-wide methylation sequencing for noninvasive prenatal, cancer, and transplantation assessments. *Proc Natl Acad Sci U S A*. 2015;112(40):E5503-12.
8. Josse J, and Husson F. missMDA: A Package for Handling Missing Values in Multivariate Data Analysis. 2016. 2016;70(1):31.
9. Ha G, Roth A, Lai D, Bashashati A, Ding J, Goya R, et al. Integrative analysis of genome-wide loss of heterozygosity and monoallelic expression at nucleotide resolution reveals disrupted pathways in triple-negative breast cancer. *Genome Res*. 2012;22(10):1995-2007.
10. Adalsteinsson VA, Ha G, Freeman SS, Choudhury AD, Stover DG, Parsons HA, et al. Scalable whole-exome sequencing of cell-free DNA reveals high concordance with metastatic tumors. *Nat Commun*. 2017;8(1):1324.
11. Lê S, Josse J, and Husson F. FactoMineR: An R Package for Multivariate Analysis. 2008. 2008;25(1):18.
12. Pedregosa F, Ga, #235, Varoquaux I, Gramfort A, Michel V, et al. Scikit-learn: Machine Learning in Python. *J Mach Learn Res*. 2011;12:2825-30.
13. Pidsley R, Zotenko E, Peters TJ, Lawrence MG, Risbridger GP, Molloy P, et al. Critical evaluation of the Illumina MethylationEPIC BeadChip microarray for whole-genome DNA methylation profiling. *Genome Biol*. 2016;17(1):208.
14. Edgar R, Domrachev M, and Lash AE. Gene Expression Omnibus: NCBI gene expression and hybridization array data repository. *Nucleic Acids Res*. 2002;30(1):207-10.
15. Fraser M, Sabelnykova VY, Yamaguchi TN, Heisler LE, Livingstone J, Huang V, et al. Genomic hallmarks of localized, non-indolent prostate cancer. *Nature*. 2017;541(7637):359-64.
16. Liberzon A, Birger C, Thorvaldsdottir H, Ghandi M, Mesirov JP, and Tamayo P. The Molecular Signatures Database (MSigDB) hallmark gene set collection. *Cell Syst*. 2015;1(6):417-25.

17. Zambelli F, Pesole G, and Pavesi G. PscanChIP: Finding over-represented transcription factor-binding site motifs and their correlations in sequences from CHIP-Seq experiments. *Nucleic Acids Res.* 2013;41(Web Server issue):W535-43.
18. Heinz S, Benner C, Spann N, Bertolino E, Lin YC, Laslo P, et al. Simple combinations of lineage-determining transcription factors prime cis-regulatory elements required for macrophage and B cell identities. *Mol Cell.* 2010;38(4):576-89.

572 **Supplementary figures**

573

574 **figure S1.** Box plot showing coverage distribution in target regions by bisulfite high-coverage next-generation
575 sequencing (NGS) in plasma samples.

576 **figure S2.** Box plot showing methylation ratio distribution for baseline (A) and progression (B) plasma samples
577 and white blood cells (C) presented separately.

578 **figure S3.** The genomic annotation based on location of methylation segments in the custom targeted panel
579 and in segments covered >10X in 19 baseline samples.

580 **figure S4.** Bland-Altman plot showing agreement for tumor fraction estimation by genomically-determined
581 tumor fraction and on LP-WGBS.

582 **figure S5.** Correlation of median methylation ratio of selected segments with genomically-determined tumor
583 fraction. Y-axis shows the correlation value and the X-axis denotes the number of top correlated segments.

584 **figure S6.** Standard deviation of methylation ratios of selected segments. Y-axis shows the standard deviation
585 and the X-axis denotes the number of top correlated segments.

586 **figure S7.** Methylation ratios of *GSTP1*, *APC*, and *RASSF1A* across different tissue types—healthy volunteer
587 plasma, white blood cells, CRPC plasma samples, LNCaP cell line.

588 **figure S8.** ct-MethSig segment methylation ratio derived from mCRPC tissues lined by tumor fraction

589 **figure S9.** Correlation between HSPC tissue tumor fraction estimation by ct-MethSig and molecularly-defined
590 tumor fraction.

591 **figure S10.** Permutation test on genes overlapping with ct-MethSig; the red dot represents the gene
592 enrichment test (GSEA) *P* value in genes overlapping with ct-MethSig and the box represents *P* values of the
593 permutation test with 1000-time iteration.

594 **figure S11.** Methylation ratio distribution of circulating normal prostate specific or prostate cancer specific
595 component in localized prostate cancer from TCGA

596 **figure S12.** Median methylation ratio of 993 MethSig3 segments positively correlated with PC3 values across
597 different sample types—plasma, white blood cells, cell lines (LNCaP, LNCaP95, VCaP), CASCADE tumor
598 (mCRPC biopsy) are plotted against the median methylation ratio of top correlated segments with ct-MethSig.

599 **figure S13.** Copy number alteration plots from LP-WGS on plasma DNA with and without bisulfite treatment

600 **figure S14.** Prevalence of gain and loss events lined by chromosome position extracted from LP-WGBS on
601 mCRPC plasma samples.

602 **figure S15.** Analysis of copy number profiles on low-pass whole genome bisulfite sequencing. Matrix shows
603 gains (red) and losses (blue) ordered by chromosomal position (columns) for individual patient samples (one
604 per row) ordered by tumor purity. Bar chart on the left shows tumor fraction per sample. Bar chart on the right
605 shows the number of gain (red) or loss (blue) events per sample.

606 **figure S16.** Manhattan plot showing the level of significance of the association between PC1 value distribution
607 and copy number alterations ordered by chromosome position. The segment containing AR is highlighted as
608 green dot (not significant, $P = 0.18$).

609 **figure S17.** Manhattan plot showing the level of significance of the association between PC3 value distribution
610 and copy number alterations ordered by chromosome position. The segment containing AR is highlighted as a
611 green dot ($P = 0.018$, Kruskal-Wallis test).

612 **figure S18.** Bland-Altman plot showing agreement between targeted methylation NGS and LP-WGBS on AR-
613 MethSig median methylation ratio

614 **figure S19.** Percentage of data to drop on different window sizes (10bps, 100bps, 1000bps, 10000bps)

615 **figure S20.** Distribution of methylation ratio by different segment size (10 bps, 100 bps, 1,000 bps, 10,000
616 bps)

617 **figure S21.** Correlation of genomically-determined tumor fraction and PC1 values derived from PCA on
618 different window sizes (10bps, 100bps, 1000bps, 10000bps)

619 **figure S22.** Performance of Gaussian Mixture Model (k-fold cross-validation, $k=100$)

620

621

622

623

624 **Supplementary Tables**

625

626 **Table S1.** Patient plasma sample characteristics.

627 **Table S2.** Targeted methylome sequencing matrix (total reads, mapped reads, % mapped reads)

628 **Table S3.** LP-WGBS matrix (total reads, mapped reads, % mapped reads)

629 **Table S4.** CASCADE patient and sample characteristics.

630 **Table S5.** Genes overlapping with AR-MethSig

631 **Table S6.** Functional enrichment of top correlated segments with principal component three

632 **Table S7.** AR-MethSig motif enrichment analysis.

633 **Table S8.** Contingency tables showing ct-MethSig and AR-MethSig segments in copy number aberrant
634 regions.

635

636

figure S1.

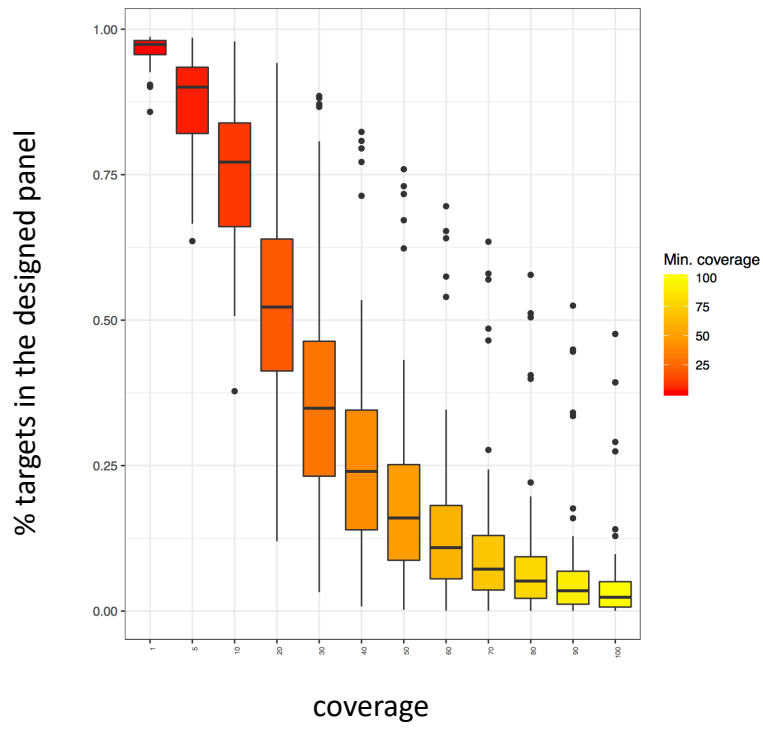


figure S2.

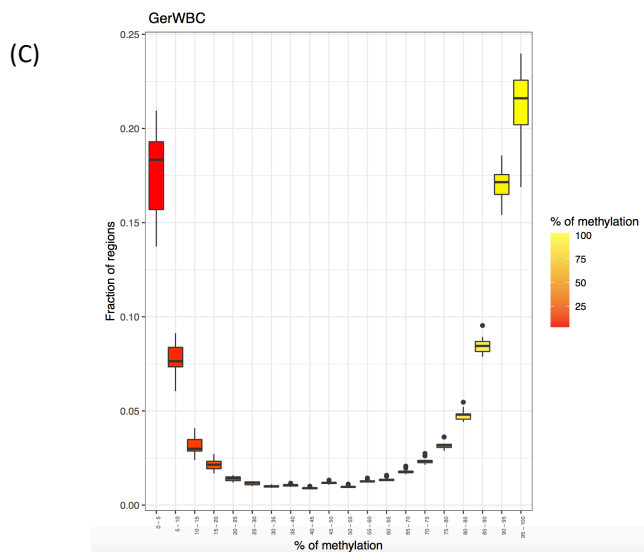
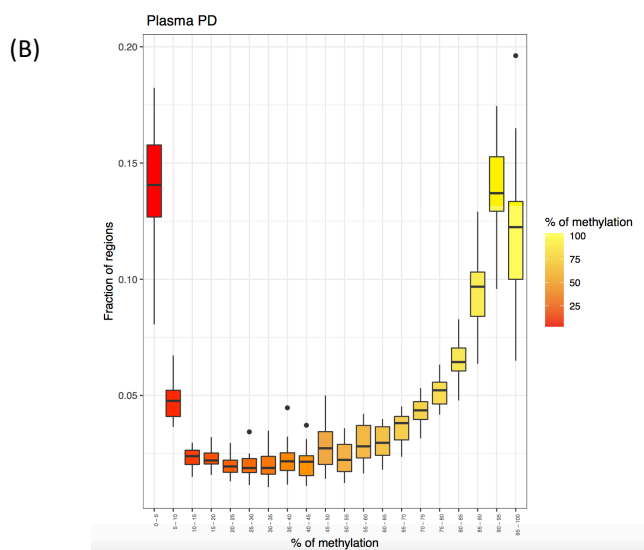
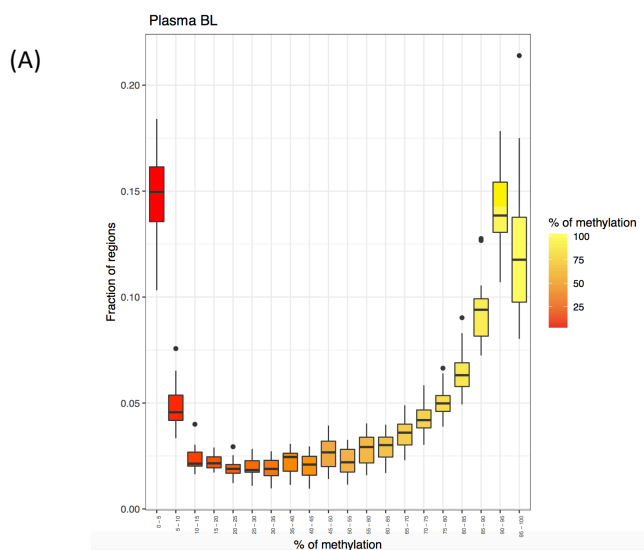


figure S3

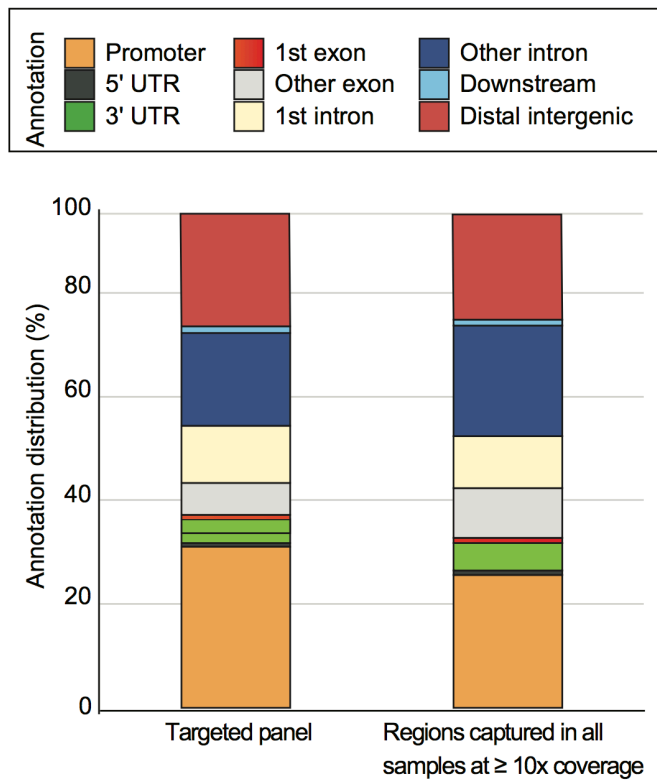
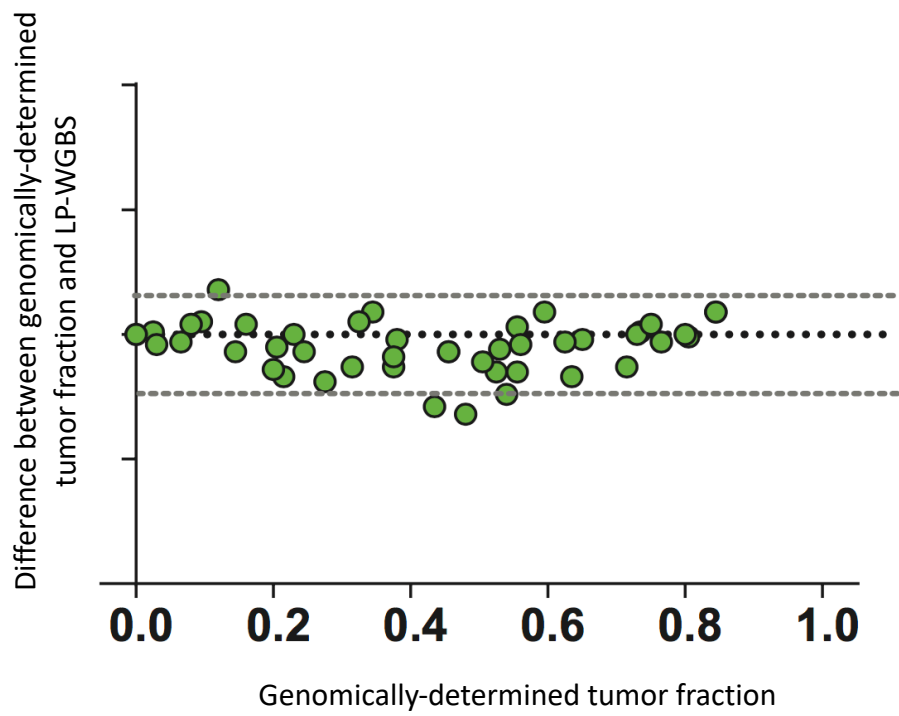


figure S4.



| | |
|--------------------------------|----------------|
| Bias | -0.0480 |
| SD of bias | 0.1028 |
| 95% Limits of Agreement | |
| From | -0.2495 |
| To | 0.1534 |

figure S5.

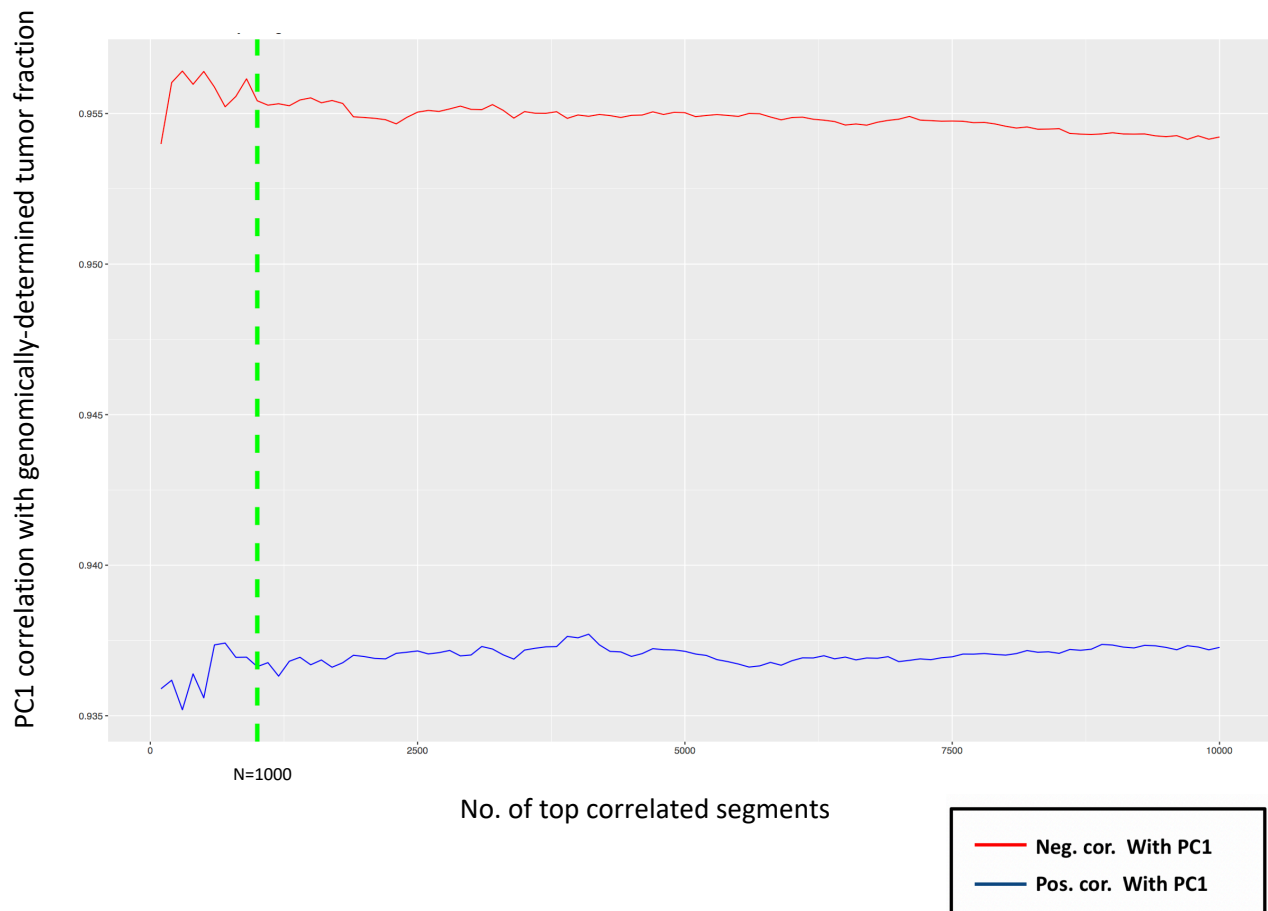


figure S6.



figure S7

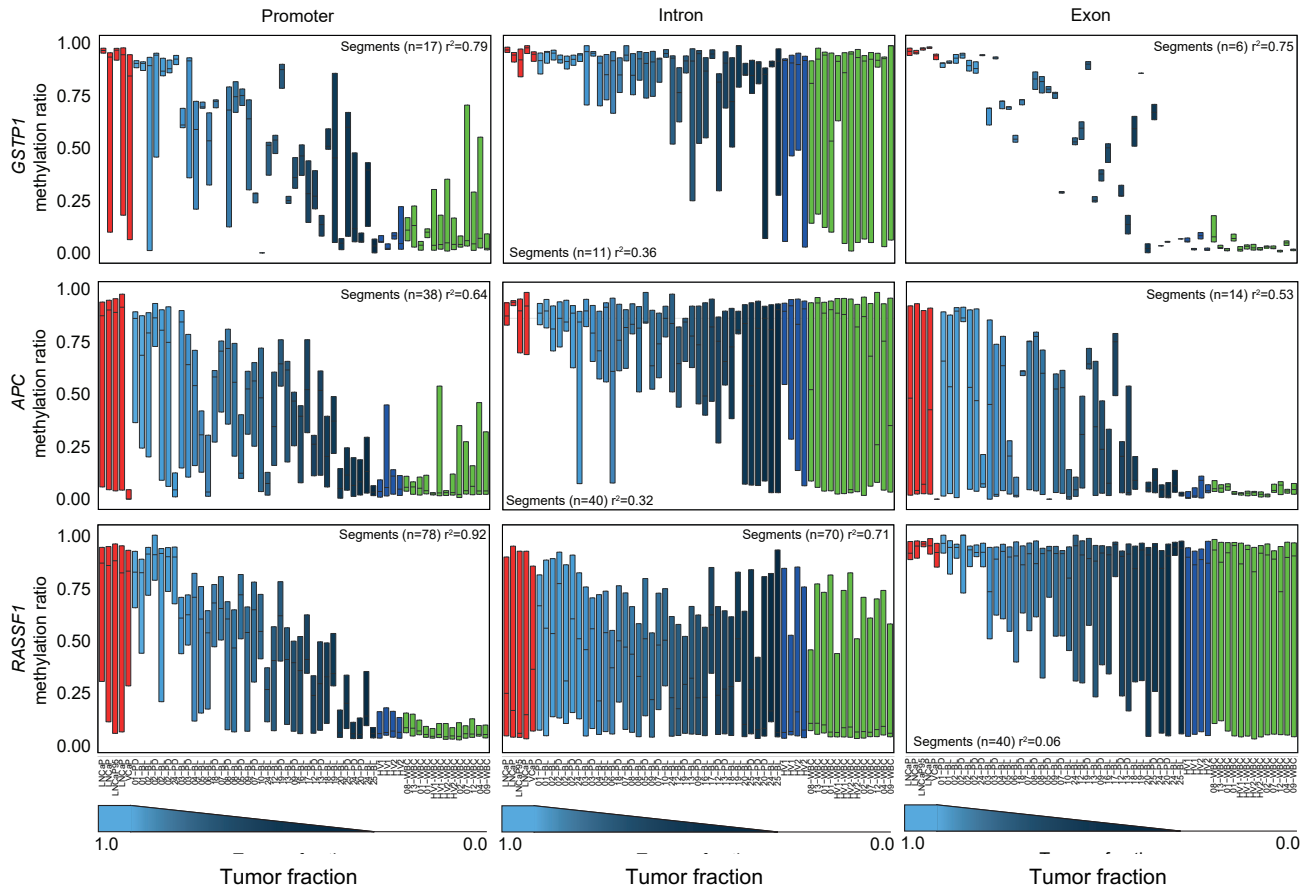
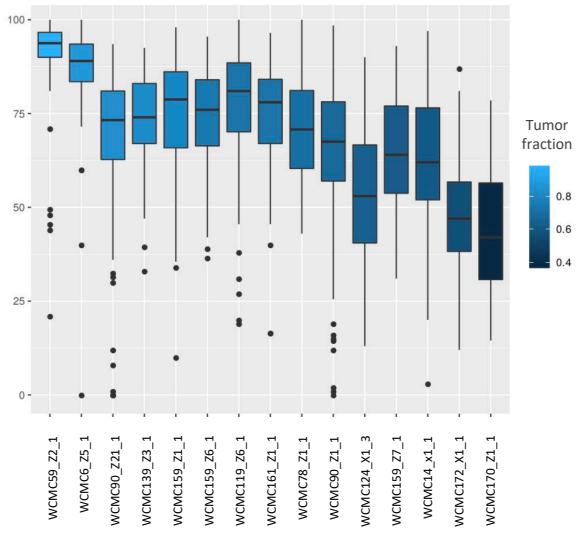


figure S8.

Top 520 segments negatively correlated with PC1



Top 480 segments positively correlated with PC1

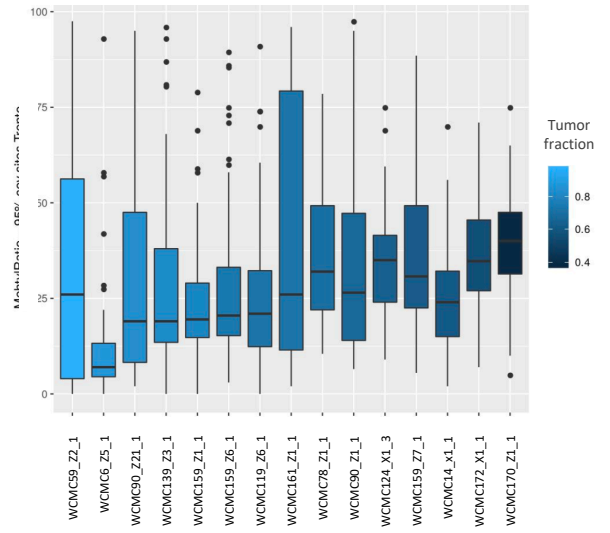


figure S9.

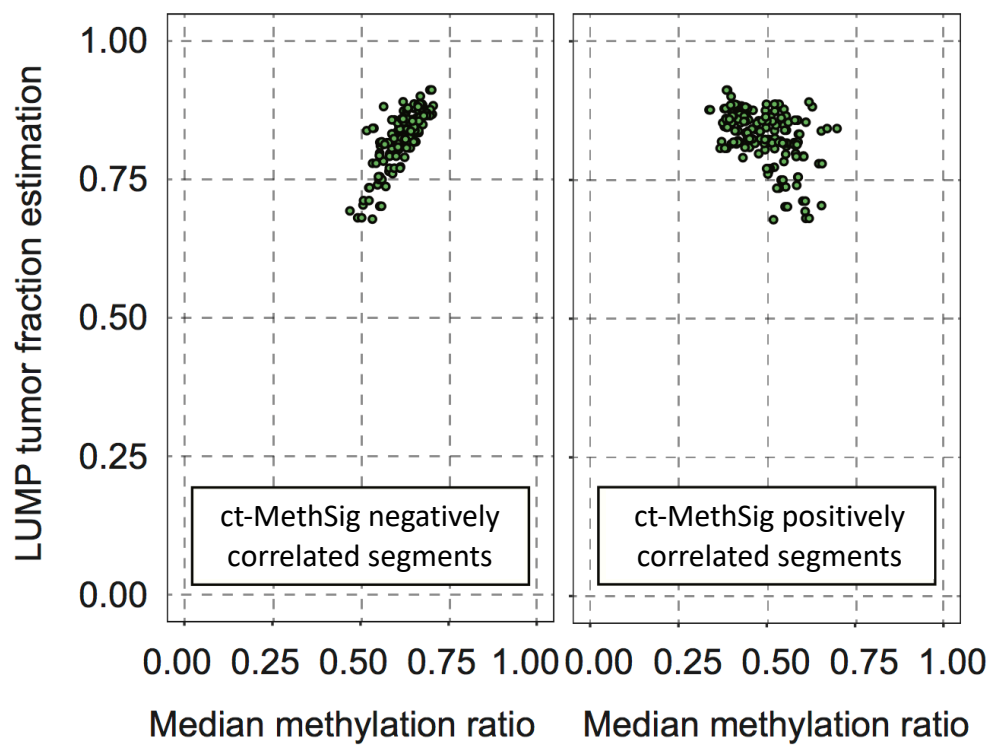


figure S10.

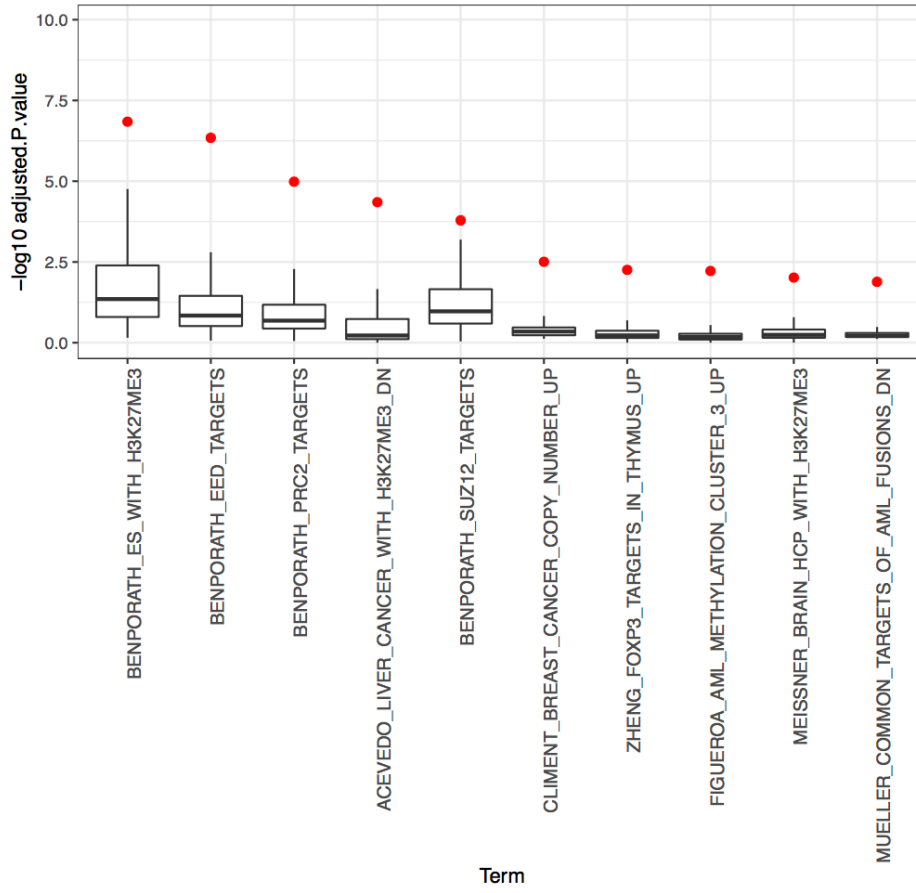
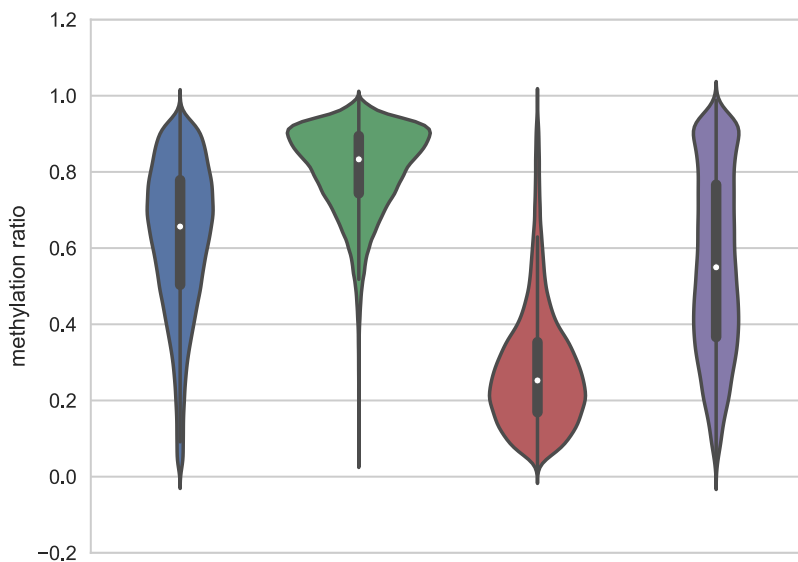


figure S11

TCGA (N = 553)



Beltran et al. (N = 12)

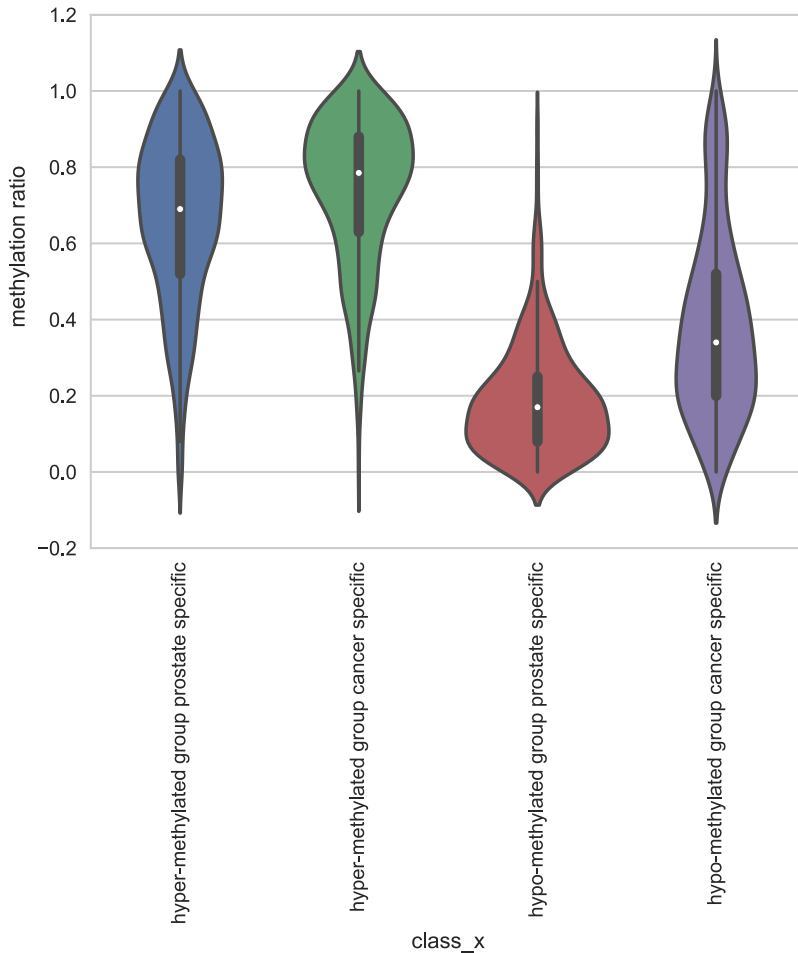


figure S12

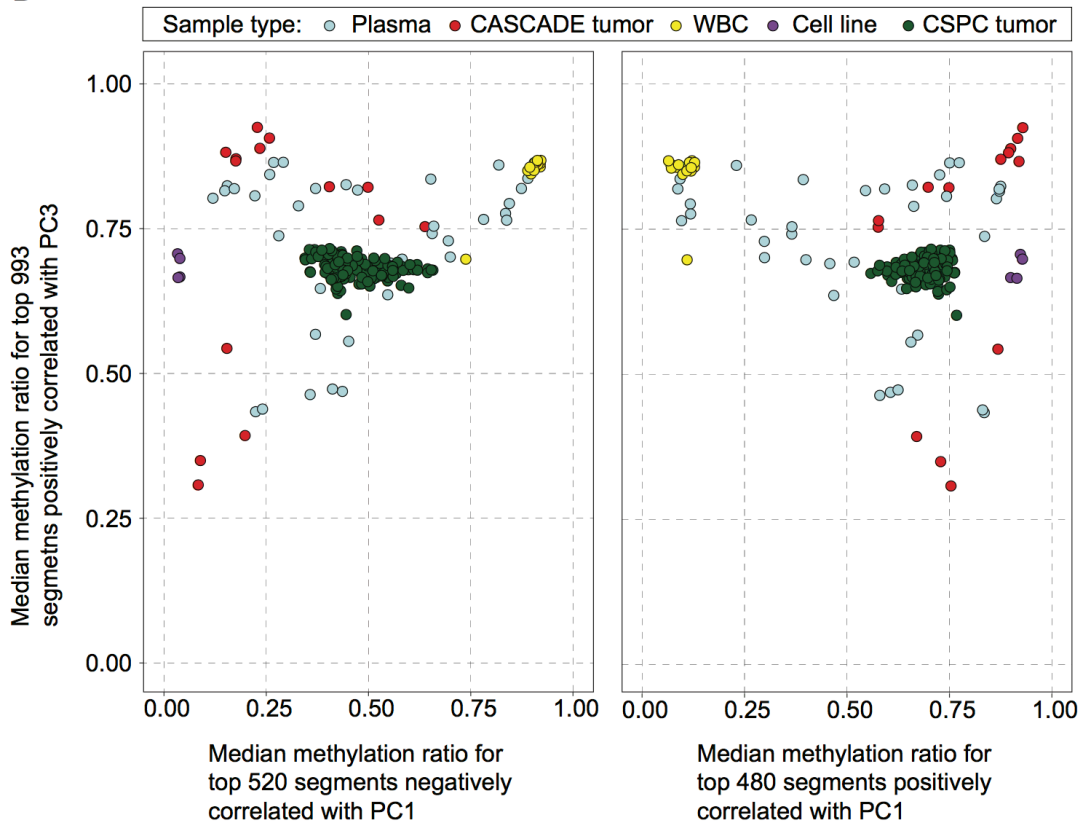


figure S13

Non bisulfite-treated

Bisulfite-treated

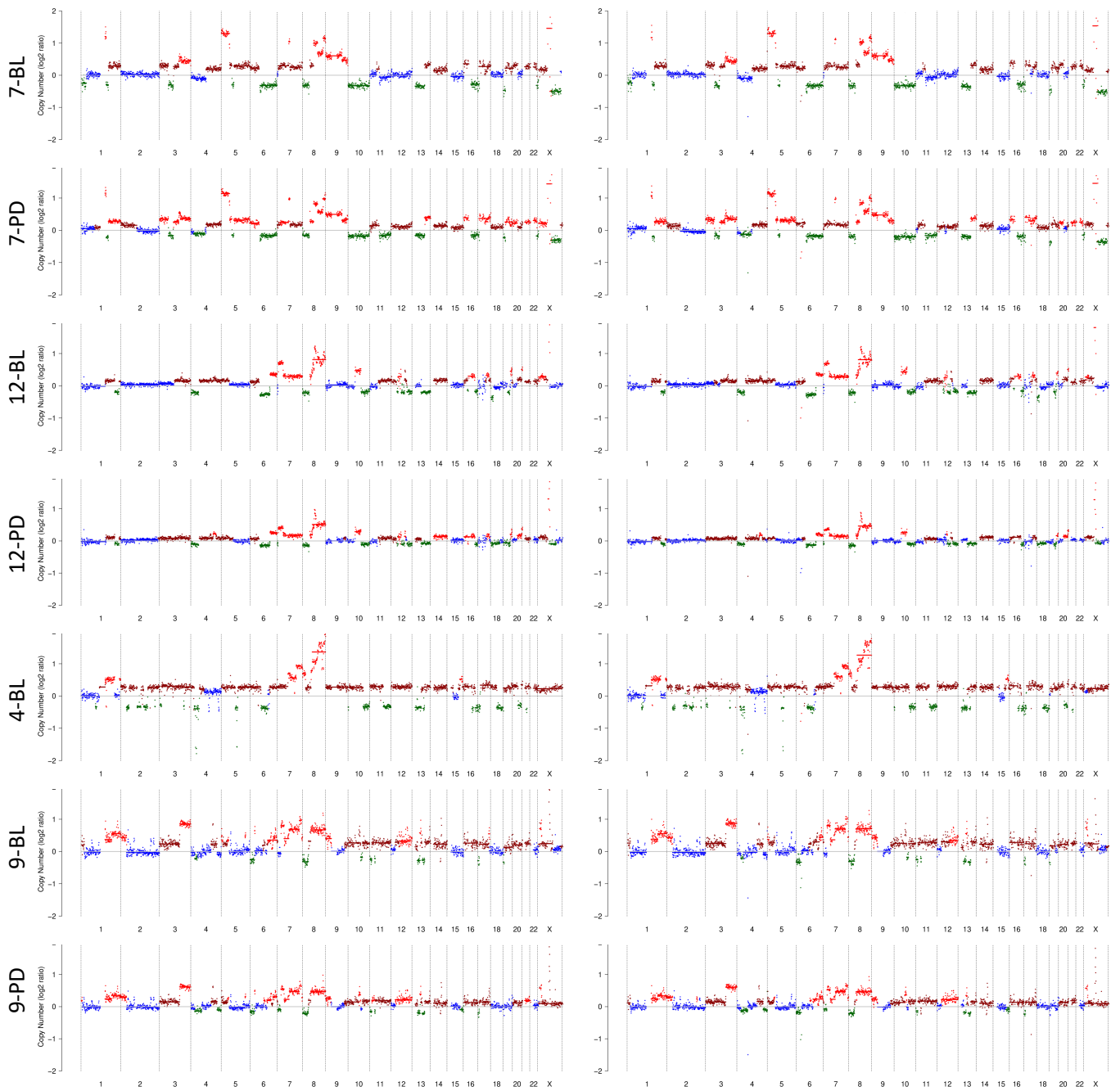


figure S14.

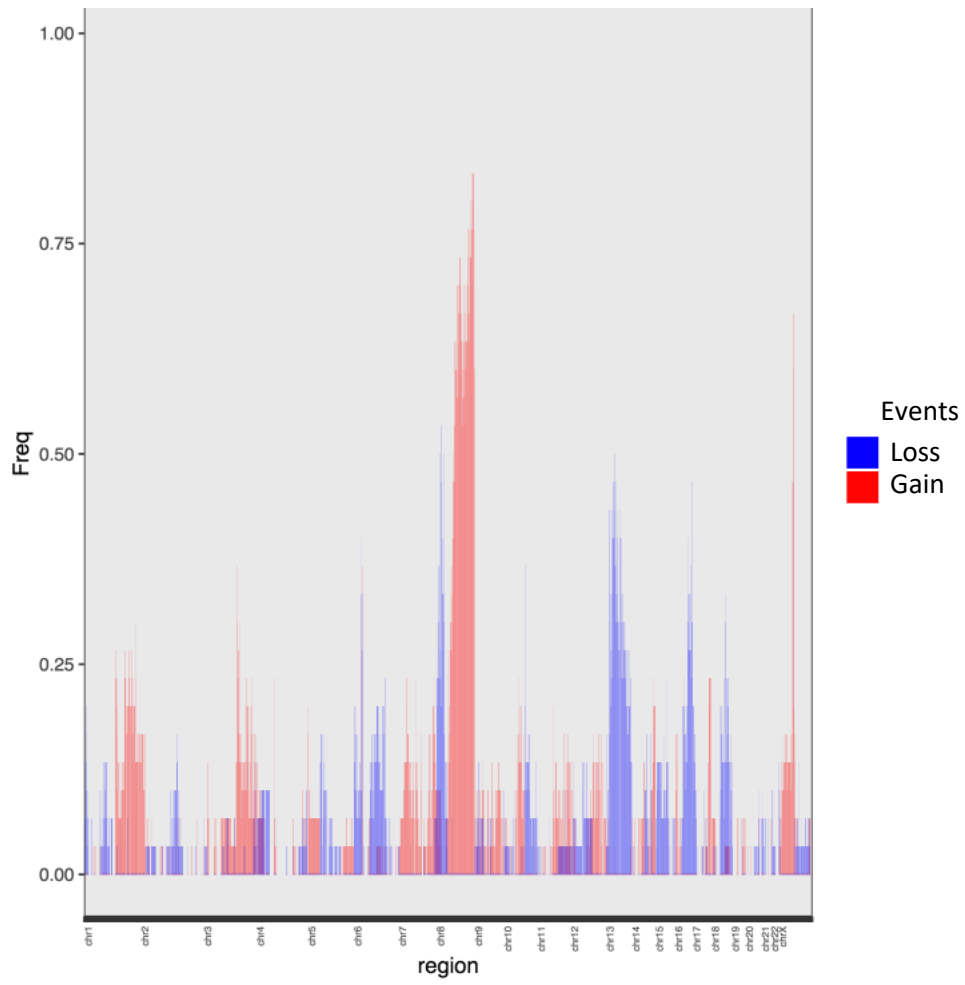


figure S16.

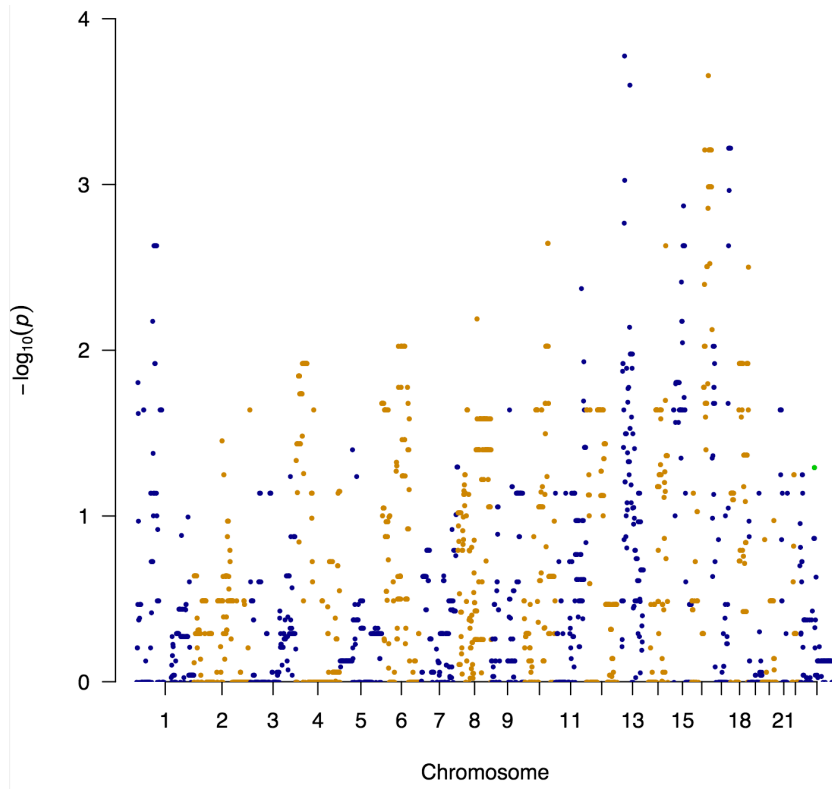


figure S17.

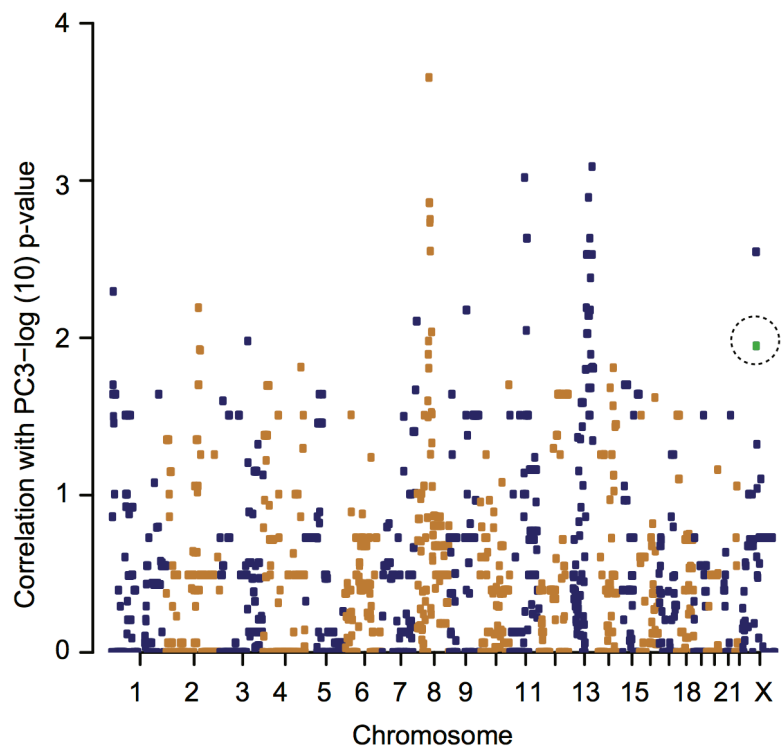
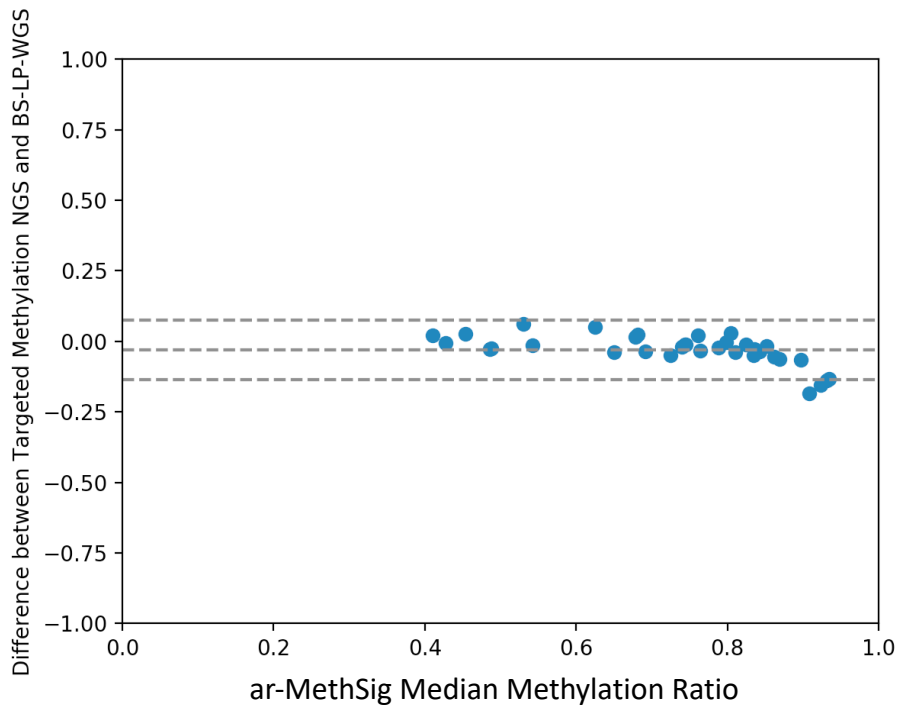


figure S18.



| | |
|--------------------------------|----------------|
| Bias | 0.029 |
| SD of bias | 0.054 |
| 95% Limits of Agreement | |
| From | - 0.136 |
| To | 0.076 |

figure S19.

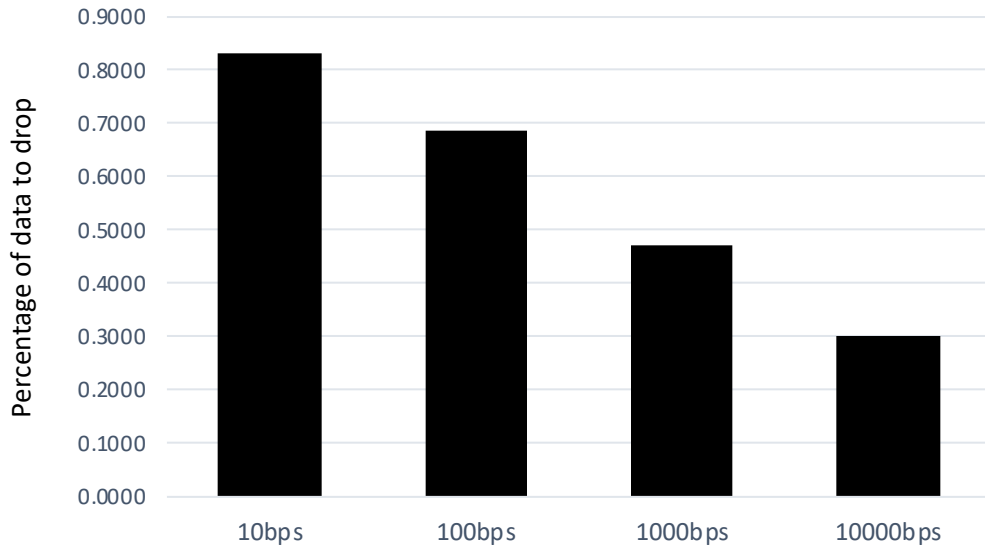


figure S20.

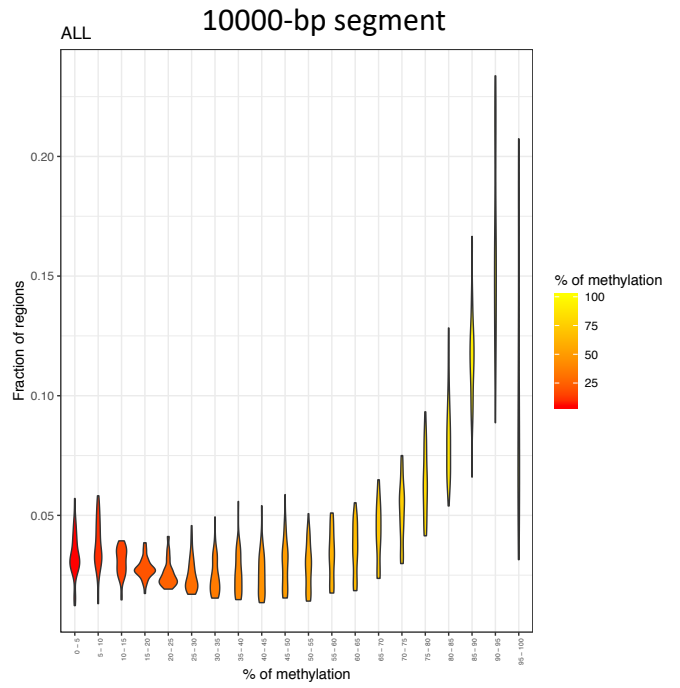
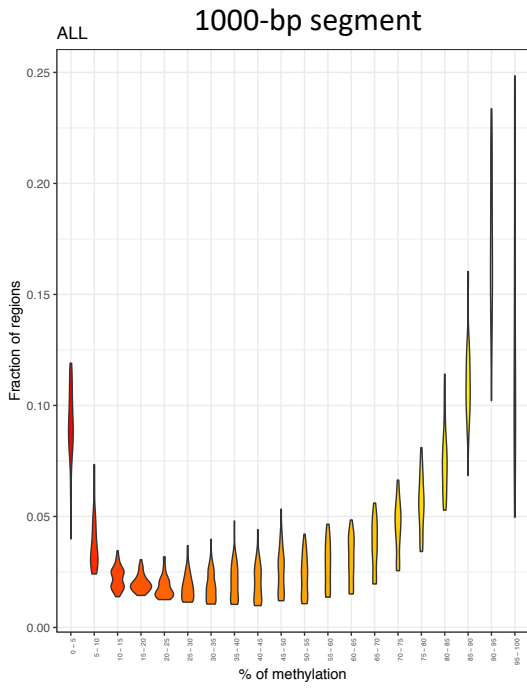
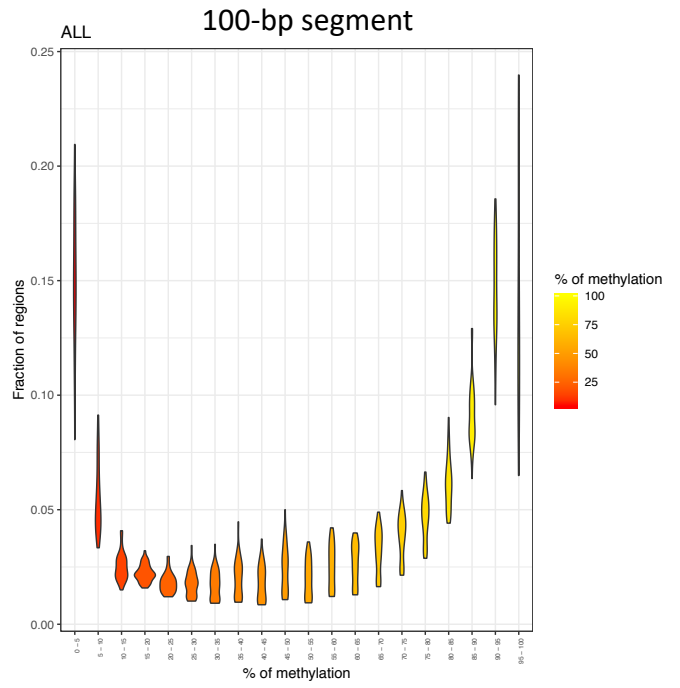
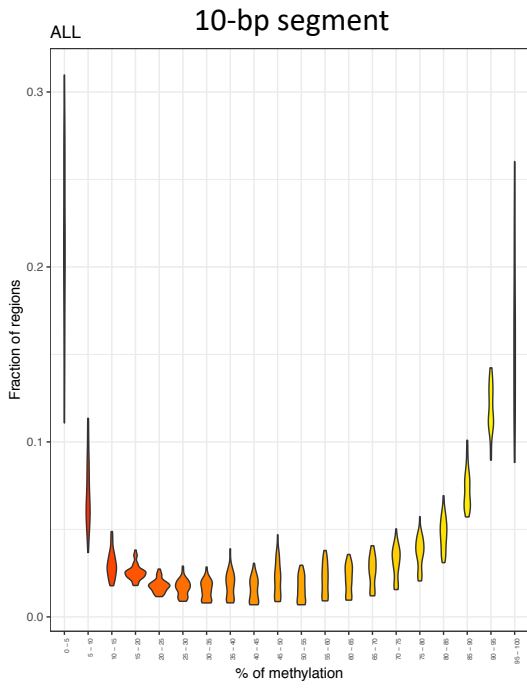
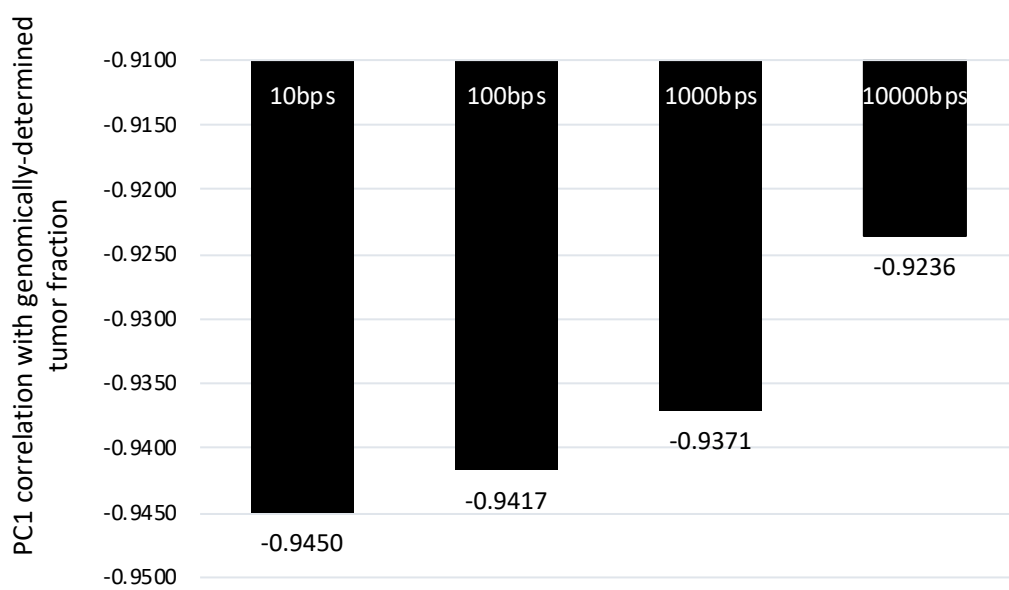
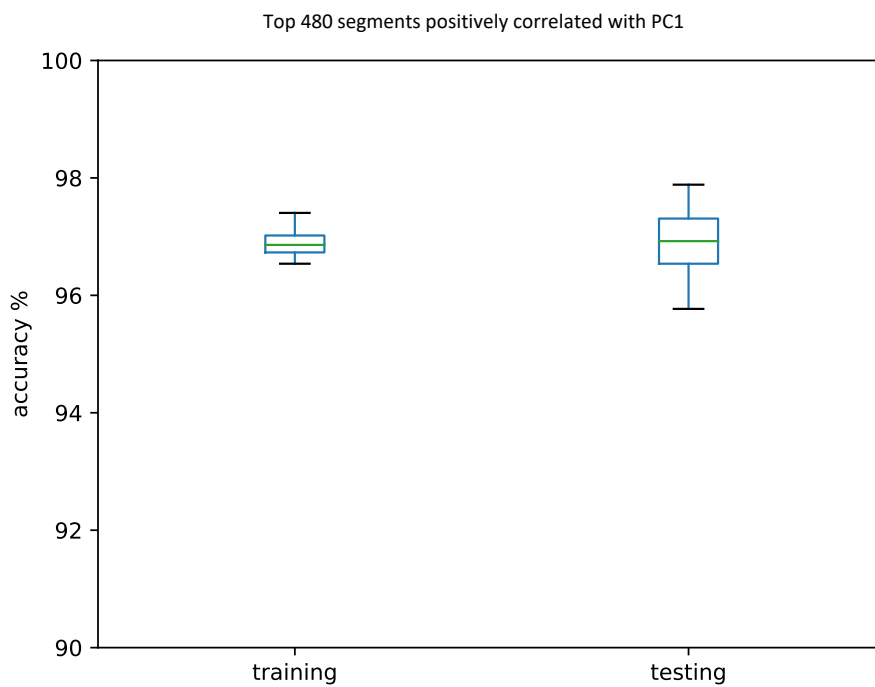
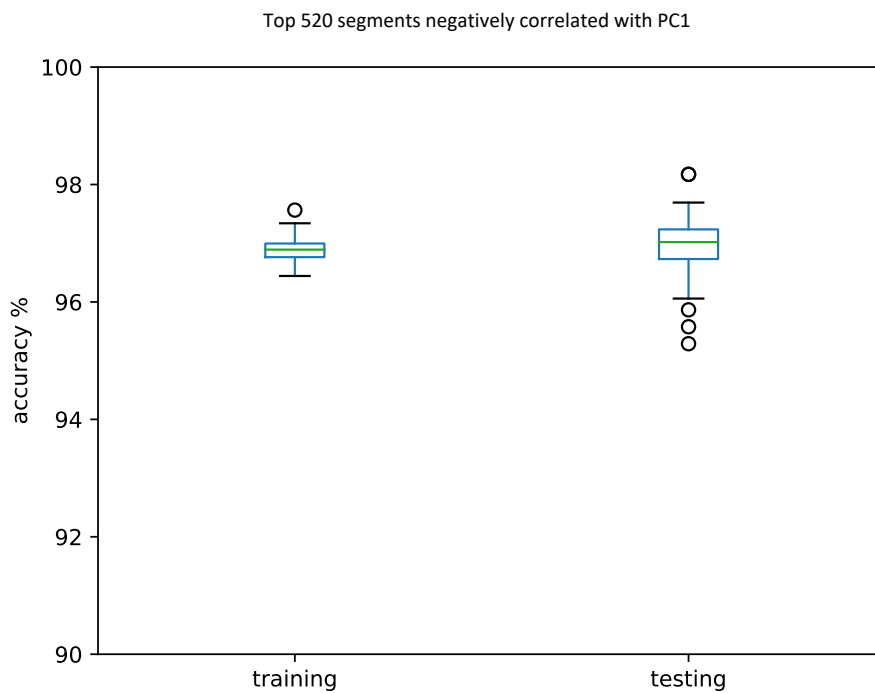


figure S21.





Supplementary Table S1

| ID | sample_type | Age | Baseline(BL) or Progression(PD) | tumor_fraction | PSA level (ng/dL) | targeted genome NGS | high_coverage WGS | targeted methylome | LP-WGBS | LP-WGS | targeted methylome on leukocytes | abiraterone (ABI) or enzalutamide (ENZ) | Start of ADT to death (months) | AR-MethSig | median methylation ratio | Sample Collection |
|-----|-------------|-----|---------------------------------|----------------|-------------------|---------------------|-------------------|--------------------|---------|--------|----------------------------------|---|--------------------------------|------------|--------------------------|-------------------|
| 1 | Plasma | 71 | BL | 0.891 | 403.5 | Yes | No | Yes | Yes | No | Yes | ABI | 14.2 | | low | IRST |
| 1 | Plasma | 71 | PD | 0.892 | 685 | Yes | No | Yes | Yes | No | Yes | ABI | 14.2 | | low | IRST |
| 2 | Plasma | 42 | BL | 0.8 | x | No | Yes | Yes | Yes | No | Yes | ABI | 59.6 | | - | Royal Marsden |
| 2 | Plasma | 42 | PD | 0.8 | 12.68 | No | Yes | Yes | Yes | No | No | ABI | 59.6 | | - | Royal Marsden |
| 3 | Plasma | 82 | BL | 0.74 | 132 | Yes | No | Yes | Yes | No | No | ABI | 55.4 | | - | IRST |
| 3 | Plasma | 82 | PD | 0.73 | 215.6 | Yes | No | Yes | Yes | No | Yes | ABI | 55.4 | | - | IRST |
| 4 | Plasma | 76 | BL | 0.65 | 67.79 | No | Yes | Yes | Yes | Yes | Yes | ENZ | 95.7 | | - | PREMIERE trial |
| 5 | Plasma | 90 | BL | 0.643 | 675.6 | Yes | No | Yes | Yes | No | No | ABI | 23.8 | | low | IRST |
| 5 | Plasma | 90 | PD | 0.477 | 611.4 | Yes | No | Yes | Yes | No | No | ABI | 23.8 | | low | IRST |
| 6 | Plasma | 80 | BL | 0.61 | 335 | Yes | No | Yes | Yes | No | No | ABI | 77.2 | | - | Royal Marsden |
| 7 | Plasma | 80 | PD | 0.45 | 20 | No | Yes | Yes | Yes | Yes | Yes | ENZ | 40.1 | | - | PREMIERE trial |
| 7 | Plasma | 80 | BL | 0.55 | 197.9 | No | Yes | Yes | Yes | Yes | No | ENZ | 40.1 | | - | PREMIERE trial |
| 8 | Plasma | 76 | BL | 0.5 | 65.12 | Yes | No | Yes | Yes | No | Yes | ABI | 25.4 | | low | IRST |
| 8 | Plasma | 76 | PD | 0.54 | 196.5 | Yes | No | Yes | Yes | No | No | ABI | 25.4 | | low | IRST |
| 9 | Plasma | 82 | PD | 0.25 | 5.73 | No | Yes | Yes | Yes | Yes | Yes | ENZ | 47.1 | | - | PREMIERE trial |
| 9 | Plasma | 82 | BL | 0.45 | 24.87 | No | Yes | Yes | Yes | Yes | No | ENZ | 47.1 | | - | PREMIERE trial |
| 10 | Plasma | 78 | BL | 0.418 | 221.4 | Yes | No | Yes | Yes | No | No | ABI | 39 | | - | IRST |
| 11 | Plasma | 66 | BL | 0.353 | 6.8 | Yes | No | No | Yes | No | No | ABI | 35.6 | | - | IRST |
| 11 | Plasma | 66 | PD | 0.64 | 6.9 | Yes | No | No | Yes | No | No | ABI | 35.6 | | - | IRST |
| 12 | Plasma | 63 | PD | 0.18 | 28.49 | No | Yes | Yes | Yes | Yes | Yes | ENZ | 20 | | - | PREMIERE trial |
| 12 | Plasma | 63 | BL | 0.325 | 33.02 | No | Yes | Yes | Yes | Yes | No | ENZ | 20 | | - | PREMIERE trial |
| 13 | Plasma | 90 | BL | 0.31 | 141.2 | Yes | No | Yes | Yes | No | Yes | ABI | 17.2 | | - | IRST |
| 13 | Plasma | 90 | PD | 0.18 | 96.1 | Yes | No | Yes | Yes | No | No | ABI | 17.2 | | - | IRST |
| 14 | Plasma | 83 | BL | 0.301 | 71.86 | Yes | No | No | Yes | No | No | ABI | 50.1 | | - | IRST |
| 14 | Plasma | 83 | PD | 0.227 | 98.43 | Yes | No | No | Yes | No | No | ABI | 50.1 | | - | IRST |
| 15 | Plasma | 70 | BL | 0.227 | 58.53 | Yes | No | No | Yes | No | No | ABI | 20.7 | | - | IRST |
| 15 | Plasma | 70 | PD | 0.013 | 6.89 | Yes | No | No | Yes | No | No | ABI | 20.7 | | - | IRST |
| 16 | Plasma | 69 | BL | 0.21 | 92 | Yes | No | Yes | Yes | No | No | ABI | 58.4 | | - | Royal Marsden |
| 17 | Plasma | 70 | BL | 0.18 | 3150 | Yes | No | Yes | Yes | No | No | ABI | 96.3 | | - | Royal Marsden |
| 18 | Plasma | 75 | BL | 0.134 | 3.5 | Yes | No | Yes | Yes | No | No | ABI | 80.9 | | - | IRST |
| 18 | Plasma | 75 | PD | 0.57 | 5.89 | Yes | No | Yes | Yes | No | No | ABI | 80.9 | | - | IRST |
| 19 | Plasma | 78 | BL | 0.128 | 126.1 | Yes | No | Yes | Yes | No | No | ABI | 29 | | low | IRST |
| 19 | Plasma | 78 | PD | 0.315 | 488.7 | Yes | No | Yes | Yes | No | No | ABI | 29 | | low | IRST |
| 20 | Plasma | 62 | BL | 0.12 | 54.26 | Yes | No | Yes | Yes | No | No | ABI | 60.1 | | - | IRST |
| 20 | Plasma | 62 | PD | 0.051 | 83.47 | Yes | No | Yes | Yes | No | No | ABI | 60.1 | | - | IRST |
| 21 | Plasma | 82 | BL | 0.096 | 69.89 | Yes | No | No | Yes | No | No | ABI | 35.5 | | - | IRST |
| 21 | Plasma | 82 | PD | 0.386 | 7.52 | Yes | No | No | Yes | No | No | ABI | 35.5 | | - | IRST |
| 22 | Plasma | 70 | BL | 0.094 | 53.83 | Yes | No | No | Yes | No | No | ABI | 49.1 | | - | IRST |
| 22 | Plasma | 70 | PD | 0.218 | 551.9 | Yes | No | No | Yes | No | No | ABI | 49.1 | | - | IRST |
| 23 | Plasma | 65 | BL | 0.046 | 25.98 | Yes | No | No | Yes | No | No | ABI | 104.5 | | - | IRST |
| 24 | Plasma | 76 | BL | 0.04 | 277 | Yes | No | Yes | No | No | Yes | ABI | 74 | | - | IRST |
| 24 | Plasma | 76 | PD | 0.09 | 50.07 | Yes | No | Yes | No | No | x | ABI | 74 | | - | IRST |
| 24 | Plasma | 76 | PD_2 | 0.354 | 684 | Yes | No | Yes | Yes | No | No | ENZ | 74 | | - | IRST |
| 24 | Plasma | 76 | PD_3 | 0.774 | 825 | Yes | No | Yes | Yes | No | No | ENZ | 74 | | - | IRST |
| 25 | Plasma | 67 | BL | 0.05 | 4.15 | Yes | No | Yes | Yes | No | No | ABI | 17.5 | | - | IRST |
| 25 | Plasma | 67 | PD | 0.086 | 2.84 | Yes | No | Yes | Yes | No | No | ABI | 17.5 | | - | IRST |
| HV1 | Plasma | 30 | HV1_R1 | 0 | x | No | No | Yes | Yes | No | Yes | x | x | | - | x |
| HV1 | Plasma | 30 | HV1_R2 | 0 | x | No | No | Yes | Yes | No | Yes | x | x | | - | x |
| HV2 | Plasma | 60 | HV2_R1 | 0 | x | No | No | Yes | No | No | Yes | x | x | | - | x |
| HV2 | Plasma | 60 | HV2_R2 | 0 | x | No | No | Yes | No | No | Yes | x | x | | - | x |

Supplementary Table S2

| ID | Baseline(BL) or Progression(PD) | sample_type | targeted methylome | Total Sequences | Mapped Reads | % Mapped Reads | % bisulfite conversion |
|-----|---------------------------------|-------------|--------------------|-----------------|--------------|----------------|------------------------|
| 1 | BL | Plasma | Yes | 186555220 | 167111560 | 89.58% | 96.6% |
| 1 | PD | Plasma | Yes | 200776658 | 179727102 | 89.52% | 96.5% |
| 2 | BL | Plasma | Yes | 65664842 | 58274518 | 88.75% | 97.0% |
| 2 | PD | Plasma | Yes | 69840940 | 62048086 | 88.84% | 97.0% |
| 3 | BL | Plasma | Yes | 152787676 | 137065257 | 89.71% | 96.7% |
| 3 | PD | Plasma | Yes | 165073482 | 147544256 | 89.38% | 96.5% |
| 4 | BL | Plasma | Yes | 294076770 | 248481849 | 84.50% | 95.4% |
| 5 | BL | Plasma | Yes | 58272348 | 51930705 | 89.12% | 96.7% |
| 5 | PD | Plasma | Yes | 46653168 | 41603630 | 89.18% | 96.6% |
| 6 | BL | Plasma | Yes | 155781620 | 135133214 | 86.75% | 97.1% |
| 7 | PD | Plasma | Yes | 78308978 | 68536718 | 87.52% | 96.5% |
| 7 | BL | Plasma | Yes | 47126584 | 39744701 | 84.34% | 96.2% |
| 8 | BL | Plasma | Yes | 168923880 | 150406167 | 89.04% | 96.6% |
| 8 | PD | Plasma | Yes | 200709408 | 178679515 | 89.02% | 96.5% |
| 9 | PD | Plasma | Yes | 290996960 | 249810225 | 85.85% | 96.5% |
| 9 | BL | Plasma | Yes | 368847482 | 318176786 | 86.26% | 96.6% |
| 10 | BL | Plasma | Yes | 48419738 | 40566381 | 83.78% | 97.1% |
| 11 | BL | Plasma | No | x | x | x | x |
| 11 | PD | Plasma | No | x | x | x | x |
| 12 | PD | Plasma | Yes | 329218080 | 279039378 | 84.76% | 96.4% |
| 12 | BL | Plasma | Yes | 92879856 | 76751623 | 82.64% | 96.2% |
| 13 | BL | Plasma | Yes | 183498796 | 164867778 | 89.85% | 96.5% |
| 13 | PD | Plasma | Yes | 201791470 | 179503148 | 88.95% | 96.6% |
| 14 | BL | Plasma | No | x | x | x | x |
| 14 | PD | Plasma | No | x | x | x | x |
| 15 | BL | Plasma | No | x | x | x | x |
| 15 | PD | Plasma | No | x | x | x | x |
| 16 | BL | Plasma | Yes | 148832250 | 128633440 | 86.43% | 97.0% |
| 17 | BL | Plasma | Yes | 136306032 | 116853097 | 85.73% | 96.9% |
| 18 | BL | Plasma | Yes | 62626728 | 55853347 | 89.18% | 96.7% |
| 18 | PD | Plasma | Yes | 51544194 | 45752062 | 88.76% | 96.8% |
| 19 | BL | Plasma | Yes | 26710136 | 23904934 | 89.50% | 97.2% |
| 19 | PD | Plasma | Yes | 32932662 | 29646068 | 90.02% | 96.9% |
| 20 | BL | Plasma | Yes | 106508740 | 95230613 | 89.41% | 96.8% |
| 20 | PD | Plasma | Yes | 120300158 | 107326545 | 89.22% | 96.7% |
| 21 | BL | Plasma | No | x | x | x | x |
| 21 | PD | Plasma | No | x | x | x | x |
| 22 | BL | Plasma | No | x | x | x | x |
| 22 | PD | Plasma | No | x | x | x | x |
| 23 | BL | Plasma | No | x | x | x | x |
| 24 | BL | Plasma | Yes | 136490762 | 121086940 | 88.71% | 96.6% |
| 24 | PD | Plasma | Yes | 150877238 | 135508492 | 89.81% | 96.6% |
| 24 | PD_2 | Plasma | Yes | 44467698 | 39895075 | 89.72% | 97.1% |
| 24 | PD_3 | Plasma | Yes | 50086012 | 44301319 | 88.45% | 96.1% |
| 25 | BL | Plasma | Yes | 57279412 | 51098610 | 89.21% | 96.5% |
| 25 | PD | Plasma | Yes | 58802244 | 52411556 | 89.13% | 96.4% |
| HV1 | HV1_R1 | Plasma | Yes | 56437928 | 51092703 | 90.53% | 96.9% |
| HV1 | HV1_R2 | Plasma | Yes | 93236514 | 82308864 | 88.28% | 96.6% |
| HV2 | HV2_R1 | Plasma | Yes | 29924470 | 27088855 | 90.52% | 96.7% |
| HV2 | HV2_R2 | Plasma | Yes | 139484410 | 123219652 | 88.34% | 96.9% |

Supplementary Table S3

| ID | Baseline(BL) or Progression(PD) | sample_type | LP-WGBS | Total Sequences | Mapped Reads | % Mapped Reads | % bisulfite conversion |
|-----|---------------------------------|-------------|---------|-----------------|--------------|----------------|------------------------|
| 1 | BL | Plasma | Yes | 61555740 | 54210537 | 88.1% | 96.6% |
| 1 | PD | Plasma | Yes | 63848530 | 55948225 | 87.6% | 96.5% |
| 2 | BL | Plasma | Yes | 42761332 | 36870167 | 86.2% | 96.0% |
| 2 | PD | Plasma | Yes | 42617996 | 36617189 | 85.9% | 96.4% |
| 3 | BL | Plasma | Yes | 59129422 | 52246290 | 88.4% | 96.7% |
| 3 | PD | Plasma | Yes | 56151334 | 49450718 | 88.1% | 96.5% |
| 4 | BL | Plasma | Yes | 66690658 | 55297446 | 82.9% | 95.4% |
| 5 | BL | Plasma | Yes | 41154970 | 35842986 | 87.1% | 96.7% |
| 5 | PD | Plasma | Yes | 42454336 | 36955379 | 87.0% | 96.6% |
| 6 | BL | Plasma | Yes | 63468228 | 54152133 | 85.3% | 97.1% |
| 7 | PD | Plasma | Yes | 58724038 | 50405549 | 85.8% | 96.5% |
| 7 | BL | Plasma | Yes | 52757540 | 44105950 | 83.6% | 96.4% |
| 8 | BL | Plasma | Yes | 48997884 | 42906582 | 87.6% | 96.6% |
| 8 | PD | Plasma | Yes | 57210482 | 50038902 | 87.5% | 96.5% |
| 9 | PD | Plasma | Yes | 62950726 | 52762980 | 83.8% | 96.5% |
| 9 | BL | Plasma | Yes | 61130412 | 51111528 | 83.6% | 96.6% |
| 10 | BL | Plasma | Yes | 63448740 | 52815910 | 83.2% | 97.1% |
| 11 | BL | Plasma | Yes | 45050378 | 37661639 | 83.6% | 95.8% |
| 11 | PD | Plasma | Yes | 50541554 | 42458690 | 84.0% | 96.0% |
| 12 | PD | Plasma | Yes | 67810208 | 55181787 | 81.4% | 96.5% |
| 12 | BL | Plasma | Yes | 52569972 | 43274790 | 82.3% | 96.4% |
| 13 | BL | Plasma | Yes | 63728198 | 56487135 | 88.6% | 96.5% |
| 13 | PD | Plasma | Yes | 58990260 | 51675897 | 87.6% | 96.4% |
| 14 | BL | Plasma | Yes | 59532904 | 49524710 | 83.2% | 96.5% |
| 14 | PD | Plasma | Yes | 54159938 | 44737438 | 82.6% | 96.8% |
| 15 | BL | Plasma | Yes | 50568866 | 42863081 | 84.8% | 96.0% |
| 15 | PD | Plasma | Yes | 53716688 | 44653610 | 83.1% | 95.9% |
| 16 | BL | Plasma | Yes | 67981380 | 58207701 | 85.6% | 97.0% |
| 17 | BL | Plasma | Yes | 77716154 | 63939783 | 82.3% | 96.9% |
| 18 | BL | Plasma | Yes | 46956924 | 40616653 | 86.5% | 96.7% |
| 18 | PD | Plasma | Yes | 40703206 | 35013233 | 86.0% | 96.7% |
| 19 | BL | Plasma | Yes | 61515246 | 52087141 | 84.7% | 97.3% |
| 19 | PD | Plasma | Yes | 67569626 | 57153038 | 84.6% | 96.9% |
| 20 | BL | Plasma | Yes | 55356132 | 48049486 | 86.8% | 96.8% |
| 20 | PD | Plasma | Yes | 50586228 | 43874943 | 86.7% | 96.7% |
| 21 | BL | Plasma | Yes | 54428970 | 44556958 | 81.9% | 96.0% |
| 21 | PD | Plasma | Yes | 49474000 | 41833481 | 84.6% | 96.0% |
| 22 | BL | Plasma | Yes | 50742732 | 40663027 | 80.1% | 96.5% |
| 22 | PD | Plasma | Yes | 59781268 | 48210928 | 80.6% | 96.5% |
| 23 | BL | Plasma | Yes | 54949210 | 45533981 | 82.9% | 96.5% |
| 24 | BL | Plasma | No | x | x | x | x |
| 24 | PD | Plasma | No | x | x | x | x |
| 24 | PD_2 | Plasma | Yes | 80786148 | 67488386 | 83.5% | 97.1% |
| 24 | PD_3 | Plasma | Yes | 36084166 | 29019487 | 80.4% | 96.1% |
| 25 | BL | Plasma | Yes | 44581236 | 38693632 | 86.8% | 96.5% |
| 25 | PD | Plasma | Yes | 45563992 | 39312802 | 86.3% | 96.4% |
| HV1 | HV1_R1 | Plasma | Yes | 61954404 | 52870463 | 85.3% | 96.9% |
| HV1 | HV1_R2 | Plasma | Yes | 80314646 | 66651587 | 83.0% | 96.6% |
| HV2 | HV2_R1 | Plasma | No | x | x | x | x |
| HV2 | HV2_R2 | Plasma | No | x | x | x | x |

Supplementary Table S4

| patient | sample_id | metastatic sites | time on ADT (month) | time from ADT to death (month) | AR-MethSig median methylation ratio |
|---------|-----------|-------------------------------------|---------------------|--------------------------------|-------------------------------------|
| CA27 | M225 | base of bladder | 51.0 | 84.0 | - |
| CA27 | M231 | spine lumbar | 51.0 | 84.0 | - |
| CA27 | M226 | dural base skull | 51.0 | 84.0 | - |
| CA27 | M219 | right adrenal gland | 51.0 | 84.0 | - |
| CA34 | M334 | Liver: right lobe A | 26.5 | 58.5 | low |
| CA34 | M336 | Liver: right lobe C | 26.5 | 58.5 | low |
| CA34 | M337 | Liver: left lobe A | 26.5 | 58.5 | low |
| CA35 | M442 | Left para-aortic lymph node track | 60.0 | 168.0 | - |
| CA35 | M442B | Left para-aortic lymph node track B | 60.0 | 168.0 | - |
| CA36 | M294 | Roof left orbit - brain | 27.0 | 66.0 | - |
| CA36 | M296 | Dura - left orbit | 27.0 | 66.0 | - |
| CA36 | M307 | Liver: right lobe deposit C | 27.0 | 66.0 | - |
| CA43 | M437 | Liver: left lobe nodule 1 | 3.0 | 34.0 | low |

Supplementary Table S5

Genes overlapping with AR-MethSig

| | | | |
|------------|-----------|-----------|-------------|
| WNT16 | NPY | CBS | TUSC5 |
| MEOX1 | CNTFR | SPTBN4 | SORCS2 |
| ASB4 | SARDH | PGLYRP2 | ADARB2 |
| FYN | PREX1 | DMKN | ADAMTSL5 |
| ZBTB32 | PTGIS | JAK1 | KLK12 |
| MAN2B2 | KCNK15 | MEGF6 | MPPED1 |
| INSRR | RUNX2 | DISC1 | TMPRSS6 |
| ELN | HS3ST3B1 | PQLC3 | SAMD11 |
| HEXB | TMEM74B | PF4 | ERC2 |
| FSTL4 | RFPL3 | ABLIM2 | GABRD |
| FOXN3 | CBFA2T3 | ANKRD33B | DNAH17 |
| HHAT | ZSCAN10 | HIST1H2AA | LRRIQ4 |
| CAMK2B | EXOC3L2 | AQP3 | PDCD1 |
| DGKG | COL5A1 | ELFN2 | KRTDAP |
| TLE2 | KHDRBS3 | MS4A8 | LINC00523 |
| SLC9A3 | NREP | PRRX2 | AJAP1 |
| KIF26A | SRPK2 | C16orf92 | ANXA6 |
| RORA | SCRN1 | ZNF180 | LINC00336 |
| SPTB | IGF2BP3 | LY6D | DNM3 |
| CNGB1 | LMX1B | C11orf85 | DLGAP2 |
| ST6GALNAC2 | MGARP | DEGS2 | CARD11 |
| EPHA8 | MAP2K5 | KLHL30 | NTRK1 |
| IGF2BP2 | ITGA11 | SFTPC | ZNF583 |
| PAG1 | BCAR3 | KCTD19 | C2CD4A |
| PKD2L2 | CDK15 | PCSK9 | SLC34A3 |
| CRYBG3 | SLC38A4 | WNT10B | SMOC1 |
| OPRK1 | GALNS | LRRN2 | RASSF9 |
| PILRA | KSR1 | MGMT | MUC2 |
| TGFB2 | ARSG | KSR2 | C1orf95 |
| BAMBI | ASGR1 | DSCAM | IGFL2 |
| HPS4 | MMEL1 | P2RY6 | PCDHGA1 |
| CACNA1I | PRDM16 | PLEKHG5 | EXOC3L4 |
| PVALB | FHAD1 | CAMTA1 | MIR548D2 |
| RIN3 | SUSD4 | NXNL1 | MIR133A2 |
| ASB2 | KCNN3 | FBXL14 | ARL2 |
| NTSR1 | MEIS1 | PRND | MIR1268A |
| CHRNA4 | GULP1 | LRRC15 | EBF2 |
| CCM2L | PTH2R | RCAN2 | PLXNA4 |
| MGRN1 | IQSEC1 | DAB1 | URAHF |
| PLLP | SLC25A26 | C2orf70 | LINC00703 |
| ZNF423 | NKD2 | SLC6A19 | LINC00162 |
| WFDC1 | ANKRD31 | LEP | LINC00705 |
| FAM189A1 | SLC17A4 | AMZ1 | ELFN1 |
| CGB | HIST1H2BA | GPR152 | MROH5 |
| ZFR2 | ANO7 | CABP4 | STEAP2-AS1 |
| BBC3 | SLC2A12 | LINC00521 | LINC00704 |
| ZNRF4 | C7orf50 | DLEU1 | LINC00689 |
| COMP | SDK1 | KBTBD11 | EMBP1 |
| VIPR2 | NTMT1 | OR51F2 | ADAM6 |
| CPVL | PARD3 | UMODL1 | DPY19L2P4 |
| CHN2 | SERPING1 | C2orf73 | ERICH1-AS1 |
| CRHR2 | GRIK4 | UCN3 | TDGF1 |
| CLIP2 | GGTLC1 | C9orf50 | MICAL3 |
| CDH23 | PLCH2 | HTR1D | ETV5 |
| EBF3 | SCN2B | TH | LINC00535 |
| RGS9 | CDH22 | PAK2 | FMN1 |
| SOD3 | NUDT22 | C9orf139 | GPR162 |
| FAM149A | CCDC3 | FUT7 | KBTBD11-OT1 |
| DNAJC4 | VENTX | AATK | CCDC177 |
| BIRC2 | TRIM36 | CCDC172 | MIR548W |
| CALCA | PITPNC1 | CAMK1D | ESPNP |
| SLC6A12 | FGD5 | URAD | TRABD2B |
| FGF1 | ODF1 | ASCL2 | TSNAX-DISC1 |
| RBP1 | KCNMA1 | B3GALT5 | |
| EFCC1 | CACNA2D3 | SLC35F3 | |
| PLCD4 | MEGF11 | ARSI | |
| NR5A2 | RADIL | TBX1 | |
| KIF17 | GDPD5 | KCNJ12 | |
| ESRRB | SCUBE1 | PIWIL3 | |
| NPY | SPON2 | C14orf180 | |

Supplementary Table S6

| Term | Type | ID | Input.numbe | Background.i | P.value | adjusted.P.value |
|--|--------|--------|-------------|--------------|----------|------------------|
| MIKKELSEN_MCV6_HCP_WITH_H3K27ME3 | MSigDB | M1954 | 28 | 431 | 3.58E-11 | 1.19E-07 |
| MARTENS_TRETINOIN_RESPONSE_UP | MSigDB | M2098 | 35 | 706 | 1.64E-10 | 2.71E-07 |
| BENPORATH_ES_WITH_H3K27ME3 | MSigDB | M10371 | 37 | 995 | 1.08E-07 | 0.000119034 |
| BENPORATH_EED_TARGETS | MSigDB | M7617 | 34 | 921 | 5.45E-07 | 0.000451695 |
| BENPORATH_SUZ12_TARGETS | MSigDB | M9898 | 32 | 924 | 5.37E-06 | 0.003561478 |
| MEISSNER_NPC_HCP_WITH_H3K4ME3_AND_H3K27ME3 | MSigDB | M1935 | 10 | 144 | 2.96E-05 | 0.016353513 |
| NAKAMURA_METASTASIS_MODEL_DN | MSigDB | M15940 | 5 | 39 | 4.58E-05 | 0.01899284 |
| MEISSNER_NPC_HCP_WITH_H3_UNMETHYLATED | MSigDB | M1936 | 20 | 487 | 4.16E-05 | 0.01899284 |
| MEISSNER_BRAIN_HCP_WITH_H3K4ME3_AND_H3K27ME3 | MSigDB | M1941 | 32 | 1035 | 5.34E-05 | 0.019656077 |
| BENPORATH_PRC2_TARGETS | MSigDB | M8448 | 22 | 594 | 8.33E-05 | 0.027602582 |

Supplementary Table S7 (con'd)

| | | | | | | | | |
|-------|-----------|-------------|-----------|-----------|-----|-------|----------|---------------------|
| chr21 | 46816526 | 46816675 + | 46816579 | 46816595 | -22 | -7 + | 0.647184 | ATGGGCGCATTGCACCT |
| chr6 | 25727226 | 25727375 + | 25727316 | 25727332 | 15 | 30 + | 0.64671 | ATGAGCATTATGAATTC |
| chr6 | 25727176 | 25727325 + | 25727316 | 25727332 | 65 | 80 + | 0.64671 | ATGAGCATTATGAATTC |
| chr14 | 106437976 | 106438125 + | 106438014 | 106438030 | -37 | -22 - | 0.646573 | TGGAATGACGGTCTTTT |
| chr3 | 64224976 | 64225125 + | 64225064 | 64225062 | -5 | 10 + | 0.645945 | GGAGACATATTTCTGCAA |
| chr22 | 32750776 | 32750825 + | 32750875 | 32750891 | 24 | 39 + | 0.645432 | AGCAGCGAGGTGAGCCA |
| chr15 | 23894726 | 23894875 + | 23894803 | 23894819 | 2 | 17 - | 0.645372 | TAAAAACAAGGTTCCCT |
| chr6 | 18990476 | 18990625 + | 18990539 | 18990555 | -12 | 3 + | 0.645367 | AAGGAGAAAGTGATATA |
| chr6 | 18990426 | 18990575 + | 18990539 | 18990555 | 38 | 53 + | 0.645367 | AAGGAGAAAGTGATATA |
| chr11 | 102216826 | 102216975 + | 102216909 | 102216925 | 8 | 23 + | 0.645244 | GGGCAAAGAGCGTCAAC |
| chr11 | 102216776 | 102216925 + | 102216909 | 102216925 | 58 | 73 + | 0.645244 | GGGCAAAGAGCGTCAAC |
| chr1 | 7408776 | 7408925 + | 7408871 | 7408887 | 20 | 35 + | 0.645074 | ACGTTCACTGTATTACG |
| chr12 | 107297176 | 107297325 + | 107297290 | 107297306 | 39 | 54 - | 0.645013 | AATTCGCCCGGACCC |
| chr5 | 149683226 | 149683375 + | 149683333 | 149683349 | 32 | 47 + | 0.644832 | GGGACCAAGTGTTCAG |
| chr14 | 104688476 | 104688625 + | 104688529 | 104688545 | -22 | -7 - | 0.644726 | GGGTTGTCTGTGGCT |
| chr14 | 104688426 | 104688575 + | 104688529 | 104688545 | -28 | 43 - | 0.644726 | GGGTTGTCTGTGGCT |
| chr16 | 84336176 | 84336325 + | 84336219 | 84336235 | -32 | -17 - | 0.644474 | GAGCCAGCTTCTCCT |
| chr9 | 129387126 | 129387275 + | 129387244 | 129387260 | 43 | 58 + | 0.644376 | AATAAGATTATGTCACG |
| chr16 | 84336226 | 84336375 + | 84336313 | 84336329 | 12 | 27 - | 0.644103 | GAAGCAATTCTTCGCG |
| chr7 | 3018226 | 3018375 + | 3018251 | 3018267 | -50 | -35 + | 0.64396 | GGGACCGGGTGCAGGC |
| chr21 | 34350976 | 34351125 + | 34351092 | 34351108 | 41 | 56 - | 0.643876 | GAGAAAGCGCTGAGCC |
| chr11 | 62100726 | 62100875 + | 62100854 | 62100870 | 53 | 68 - | 0.643717 | CAGCCGTTGTGTGCT |
| chr10 | 26501976 | 26502125 + | 26502035 | 26502051 | -16 | -1 - | 0.643475 | GGGTGCCCTTGGCTCCT |
| chr16 | 49530526 | 49530675 + | 49530618 | 49530634 | 17 | 32 + | 0.642854 | GCGTACGGCAAATGCTC |
| chr10 | 134662176 | 134662325 + | 134662230 | 134662246 | -21 | -6 - | 0.642764 | CAGCCACTCGGCCCC |
| chr19 | 18902576 | 18902725 + | 18902648 | 18902664 | -3 | 12 - | 0.64255 | GAGTTGTCTGTATGTC |
| chr3 | 55931376 | 55931525 + | 55931438 | 55931454 | -13 | 2 + | 0.642216 | ACAGACAGGCTCTCTG |
| chr3 | 55931326 | 55931475 + | 55931438 | 55931454 | 37 | 52 + | 0.642216 | ACAGACAGGCTCTCTG |
| chr17 | 7082926 | 7083075 + | 7082967 | 7082983 | -34 | -19 - | 0.642192 | TGGAACATTGGTGCT |
| chr17 | 7082876 | 7083025 + | 7082967 | 7082983 | 16 | 31 - | 0.642192 | CAGAACATTGGTGCT |
| chr19 | 554776 | 554825 + | 554842 | 554858 | -9 | 6 + | 0.642164 | TGGAACATTTTTACAA |
| chr5 | 1010826 | 1010975 + | 1010870 | 1010886 | -31 | -16 + | 0.642158 | AGCAGCCAGGTGCTCCT |
| chr5 | 1010776 | 1010925 + | 1010870 | 1010886 | 19 | 34 + | 0.642158 | AGCAGCCAGGTGCTCCT |
| chr5 | 532876 | 533025 + | 532883 | 532899 | -68 | -53 - | 0.642064 | GGGAGCCCCGCTTGC |
| chr5 | 532826 | 532975 + | 532883 | 532899 | -18 | -3 - | 0.642064 | GGGAGCCCCGCTTGC |
| chr11 | 68781826 | 68781975 + | 68781929 | 68781945 | 28 | 43 - | 0.642048 | TGGAACCTTGTTTACAA |
| chr5 | 2207026 | 2207175 + | 2207153 | 2207169 | 52 | 67 + | 0.641807 | AAGAACCTTGTATGTC |
| chr10 | 34496226 | 34496375 + | 34496243 | 34496259 | -58 | -43 + | 0.64133 | CAGCAGCAAGTGTTCCT |
| chr11 | 69706726 | 69706875 + | 69706755 | 69706771 | -46 | -31 - | 0.641327 | TGGACAGTAAGGTGCCCT |
| chr16 | 876026 | 876175 + | 876060 | 876076 | -41 | -26 + | 0.641287 | GGTAAGATATTTTGCTG |
| chr7 | 45188076 | 45188225 + | 45188209 | 45188225 | 58 | 73 - | 0.641082 | TGGAACCTTGTTTACAA |
| chr3 | 72704626 | 72704775 + | 72704664 | 72704680 | -37 | -22 + | 0.640834 | CGGACAATTTGAACCTG |
| chr3 | 72704576 | 72704725 + | 72704664 | 72704680 | 13 | 28 + | 0.640834 | CGGACAATTTGAACCTG |
| chr11 | 1102426 | 1102575 + | 1102502 | 1102518 | 1 | 16 + | 0.640689 | ACAGACGCACTGTATCA |
| chr10 | 3500076 | 3500225 + | 3500085 | 3500101 | -66 | -51 - | 0.640501 | TGTCAACACTGAGATC |
| chr8 | 700076 | 700225 + | 700117 | 700133 | -34 | -19 + | 0.640471 | TGGAAGGGCTTTTCTCCT |
| chr8 | 700026 | 700175 + | 700117 | 700133 | 16 | 31 + | 0.640471 | TGGAAGGGCTTTTCTCCT |
| chr1 | 57718926 | 57719075 + | 57718936 | 57718952 | -65 | -50 + | 0.640099 | AGTGAAGTGTAGTTCTA |
| chr10 | 3378976 | 3379125 + | 3379045 | 3379061 | -6 | 9 + | 0.640078 | GGATAAAAAGCTGACCCG |
| chr5 | 4933226 | 4933375 + | 493331 | 493347 | 30 | 45 + | 0.640041 | GGGATAAGTGAAGTCTTCT |
| chr12 | 52238576 | 52238725 + | 52238616 | 52238632 | -35 | -20 - | 0.639402 | AGGCTGGCTAGTGCCCT |
| chr12 | 52238526 | 52238675 + | 52238616 | 52238632 | 15 | 30 - | 0.639402 | AGGCTGGCTAGTGCCCT |
| chr20 | 4705126 | 4705275 + | 4705200 | 4705216 | -1 | 14 + | 0.639337 | AGGAAGCACTGAGCTG |
| chr21 | 43547726 | 43547875 + | 43547815 | 43547831 | 14 | 29 + | 0.639049 | GAGAACGGCAACTCCAA |
| chr21 | 43547676 | 43547825 + | 43547815 | 43547831 | -4 | 79 + | 0.639049 | GAGAACGGCAACTCCAA |
| chr10 | 131650676 | 131650825 + | 131650748 | 131650764 | -3 | 12 + | 0.639019 | AGGCACTGGGATTTTCT |
| chr10 | 131650626 | 131650775 + | 131650748 | 131650764 | 47 | 62 + | 0.639019 | AGGCACTGGGATTTTCT |
| chr15 | 29037776 | 29037925 + | 29037825 | 29037841 | -26 | -11 + | 0.638952 | TGAAAAATATTTTCTGCT |
| chr16 | 22775926 | 22776075 + | 22775935 | 22775951 | -66 | -51 - | 0.638545 | AAGAAAGCTACCTTCTGCT |
| chr13 | 28563576 | 28563725 + | 28563659 | 28563675 | 8 | 23 + | 0.638529 | TGGACTCCAGTGATCA |
| chr8 | 144854576 | 144854725 + | 144854635 | 144854651 | -32 | -17 + | 0.638481 | TGTACGACAGAGGACGG |
| chr16 | 29267676 | 29267825 + | 29267809 | 29267825 | 58 | 73 - | 0.638456 | CAAGACATGGGCTTTGCT |
| chr16 | 281276 | 281425 + | 281395 | 281411 | 44 | 59 - | 0.638354 | GAGAAAGCACGTTTCTC |
| chr9 | 6716226 | 6716375 + | 6716229 | 6716245 | -72 | -57 - | 0.637996 | CGTTCTCCGTTTCCCC |
| chr11 | 120764426 | 120764575 + | 120764566 | 120764582 | 65 | 80 - | 0.637708 | TGTTAATCTCTGACCC |
| chr17 | 75848676 | 75848825 + | 75848780 | 75848796 | 29 | 44 + | 0.637621 | TGGACAGCAGCGCTGCT |
| chr6 | 37014476 | 37014625 + | 37014488 | 37014504 | -63 | -48 + | 0.637451 | AGGTAATAAAGTGCAT |
| chr12 | 107297076 | 107297225 + | 107297205 | 107297221 | -54 | 69 + | 0.637419 | GACCACCACTGCTCCT |
| chr19 | 47735626 | 47735775 + | 47735663 | 47735679 | -38 | -23 - | 0.637263 | TAGAAGAACTGACCAC |
| chr21 | 42219676 | 42219825 + | 42219774 | 42219790 | 23 | 38 + | 0.637235 | AGGGCTGGAATGACCC |
| chr9 | 132383226 | 132383375 + | 132383319 | 132383335 | 18 | 33 - | 0.636975 | AATGACAGCACTGCCT |
| chr5 | 1207376 | 1207525 + | 1207505 | 1207521 | 54 | 69 + | 0.636696 | GGGCGAGTGGAGTTCAT |
| chr1 | 210612176 | 210612325 + | 210612291 | 210612307 | 40 | 55 + | 0.636369 | GTTCACTATGATCAG |
| chr5 | 141993176 | 141993325 + | 141993205 | 141993221 | -46 | -31 + | 0.635971 | GGGGCCAGATCTTTCAC |
| chr20 | 1164876 | 1165025 + | 1164996 | 1165012 | 45 | 60 - | 0.635741 | AGTTACACAAGGCGCT |
| chr16 | 1198576 | 1198725 + | 1198634 | 1198650 | -17 | -2 - | 0.635465 | TAGACGGCTGTCAC |
| chr16 | 1198526 | 1198675 + | 1198634 | 1198650 | 33 | 48 - | 0.635465 | TAGACGGCTGTCAC |
| chr4 | 3690826 | 3690975 + | 3690909 | 3690925 | 8 | 23 + | 0.635187 | AAGAGGGGTGTGGTC |
| chr5 | 162997826 | 162997975 + | 162997853 | 162997869 | -48 | -33 - | 0.635128 | AACTATAAAATTTGCTT |
| chr7 | 104897076 | 104897225 + | 104897083 | 104897099 | -68 | -53 - | 0.63478 | AATGAGCCACTGTGCTC |
| chr17 | 74581226 | 74581375 + | 74581260 | 74581276 | -41 | -26 + | 0.634143 | GGGCGGGGGCGGACAG |
| chr3 | 97542226 | 97542375 + | 97542278 | 97542294 | -23 | -8 - | 0.633344 | TGTTCTCGGTTTCCCC |
| chr15 | 101807276 | 101807425 + | 101807394 | 101807410 | 43 | 58 - | 0.633264 | GGGTAACCTCTTTGCTT |
| chr11 | 128796326 | 128796475 + | 128796399 | 128796415 | -2 | 13 - | 0.633221 | GGCAAACTTCACTCCT |
| chr3 | 185866476 | 185866625 + | 185866549 | 185866565 | -2 | 13 - | 0.632817 | GAGTTCTCGGTTCTTCT |
| chr19 | 47735676 | 47735825 + | 47735704 | 47735720 | -47 | -32 - | 0.632121 | TGTACAGCTTCTGCTC |
| chr5 | 173737976 | 173738125 + | 173738067 | 173738083 | 16 | 31 + | 0.631909 | GGGGTGGGAGGTTCCA |
| chr11 | 2210126 | 22101415 + | 2210148 | 2210164 | -53 | -38 - | 0.631714 | GAGAAATCAGAGCCCTC |
| chr14 | 101128326 | 101128475 + | 101128332 | 101128348 | -69 | -54 - | 0.631607 | AAAAGCACCTAGACCT |
| chr14 | 101128276 | 101128425 + | 101128332 | 101128348 | -19 | -4 - | 0.631607 | AAAAGCACCTAGACCT |
| chr10 | 3572226 | 3572375 + | 3572334 | 3572350 | 33 | 48 + | 0.631352 | TGGGAAAGTCAGACCTC |
| chr15 | 99087976 | 99088125 + | 99088072 | 99088088 | 21 | 36 + | 0.631206 | TGACCATGAATACCA |

Supplementary Table S7 (con'd)

Table with 10 columns: chromosome, ID, ID, ID, ID, ID, ID, ID, ID, ID. The table lists genomic coordinates and identifiers for various chromosomes, including chr2, chr16, chr17, chr12, chr10, chr11, chr16, chr4, chr17, chr4, chr6, chr13, chr2, chr22, chr14, chr3, chr3, chr7, chr10, chr2, chr4, chr17, chr22, chr16, chr19, chr7, chr7, chr10, chr12, chr12, chr19, chr17, chr20, chr1, chr4, chr10, chr1, chr14, chr22, chr19, chr19, chr15, chr6, chr1, chr10, chr17, chr12, chr8, chr6, chr12, chr5, chr11, chr21, chr1, chr4, chr2, chr9, chr5, chr22, chr5, chr5, chr10, chr7, chr4, chr5, chr14, chr12, chr1, chr5, chr19, chr8, chr5, chr13, and chr6. Each row contains specific genomic coordinates and identifiers for each chromosome.

Supplementary Table S8

| | copy number aberration (CNA) regions | non-CNA regions |
|--------------|--------------------------------------|-----------------|
| ct-MethSig | 35 | 965 |
| All segments | 1031 | 236479 |
| ar-MethSig | 0 | 1000 |
| All segments | 1031 | 236479 |